NRC Research Press

REVIEW

Recent developments in the study of insect flight[1]

Tyson L. Hedrick, Stacey A. Combes, and Laura A. Miller

Abstract: Here we review recent contributions to the study of insect flight, in particular those brought about by advances in experimental techniques. We focus particularly on the following areas: wing flexibility and deformation, the physiology and biophysics of asynchronous insect flight muscle, the aerodynamics of flight, and stability and maneuverability. This recent research reveals the importance of wing flexibility to insect flight, provides a detailed model of how asynchronous flight muscle functions and how it may have evolved, synthesizes many recent studies of insect flight aerodynamics into a broad-reaching summary of unsteady flight aerodynamics, and highlights new insights into the sources of flight stability in insects. The focus on experimental techniques and recently developed apparatus shows how these advancements have occurred and point the way towards future experiments.

Key words: Insecta, flight, biomechanics, biophysics, physiology, locomotion, morphology.

Résumé : Nous passons en revue les contributions récentes à l'étude du vol des insectes, particulièrement celles qui découlent d'avancées au plan des méthodes expérimentales. Nous mettons l'accent sur les domaines suivants : la flexibilité et la déformation des ailes, la physiologie et la biophysique des muscles asynchrones du vol des insectes, l'aérodynamique du vol et la stabilité et la manœuvrabilité. Ces travaux récents révèlent l'importance de la flexibilité des ailes pour le vol des insectes, fournissent un modèle détaillé du fonctionnement des muscles asynchrones du vol et de l'évolution possible de ce fonctionnement, intègrent de nombreuses études récentes de l'aérodynamique du vol des insectes en un sommaire d'une grande portée des insectes présentant une aérodynamique de vol instationnaire et font ressortir les nouvelles connaissances sur les sources de stabilité du vol chez les insectes. L'examen des méthodes expérimentales et d'appareils mis au point récemment illustre comment ces avancées se sont produites et indique des avenues pour des expériences futures. [Traduit par la Rédaction]

Mots-clés : insectes, vol, biomécanique, biophysique, physiologie, locomotion, morphologie.

Introduction

Over the past 14 years, scientific understanding of insect flight has been substantially altered by the appearance of new experimental techniques for measuring everything from the aerodynamics of flight to the movement of actin and myosin proteins within insect flight muscle and the flight control responses of freely flying animals. The information revealed by these new approaches has cascaded through the entire field of insect flight, revising long-held assumptions and changing the interpretation of prior results. Here we review recent contributions to the understanding of insect flight in the areas of wing anatomy and structure, muscle physiology and the energetics of flight, the aerodynamics of insect flight, and sensing and flight control.

Wing morphology and flexibility

Insect wings are complex, deformable structures that change shape continuously during flight. While some insects can modulate wing shape to a limited extent via muscles inserting on different portions of the wing base (e.g., hind wing "umbrella" extension in locusts and alula actuation in hover flies; Wootton et al. 2000; Walker et al. 2012), most deformations in flapping insect wings are passive. Deformations are difficult to predict or model because the instantaneous wing shape is determined not only by the complex architecture of the wing but also by interactions between flight forces (i.e., intrinsic, aerodynamic, and inertial). The modeling challenge is further compounded when aeroelasticity, the mutual interaction between aerodynamic forces and wing shape, is considered. However, evidence is accumulating from both experimental and theoretical studies that inertial deformation overshadows aeroelastic deformation in determining instantaneous wing shape (Ennos 1988; Daniel and Combes 2002; Combes and Daniel 2003*c*; Bergou et al. 2007).

Quantifying deformation

Insect wing deformations vary enormously between species, during different types of flight, and even from stroke to stroke, although general patterns of bending during the stroke cycle can be identified. During the downstroke, the wings of most insects are relatively flat, often with a slight camber or twist. At supination, the transition from downstroke to upstroke, the leading edge stops moving forward relative to the body and rotates to move backwards and up. Most insect wings display some degree of ventral flexion during supination, with the tip or even the whole wing bending forward and down (e.g., Figs. 1A, 1B, 1C, 1H). Some

Received 19 August 2013. Accepted 25 August 2014.

T.L. Hedrick.* Department of Biology, University of North Carolina at Chapel Hill, Chapel Hill, NC 27599, USA.
S.A. Combes.*,† Harvard University, Concord Field Station, 100 Old Causeway Road, Bedford, MA 01730, USA.
L.A. Miller.* Departments of Mathematics and Biology, University of North Carolina at Chapel Hill, Chapel Hill, NC 27599, USA.
Corresponding author: Tyson L. Hedrick (e-mail: thedrick@bio.unc.edu).
*These authors contributed equally to this review.
†Present address: Department of Neurobiology, Physiology, and Behavior, University of California Davis, Davis, CA 95616, USA.

[1]This review is part of a virtual symposium entitled "Advances in animal flight studies" that presents perspectives on improved understanding of the biology of flight in gliding animals, insects, pterosaurs, birds, and bats.

Fig. 1. Dynamic wing bending in flying insects: (A–D) bees and wasps; (E–H) butterflies and moths. (From Nachtigall 2000; reproduced with permission of Entomol. Gen., vol. 25, issue 1, ©2000 E. Schweizerbart'sche Verlagsbuchhandlung.)

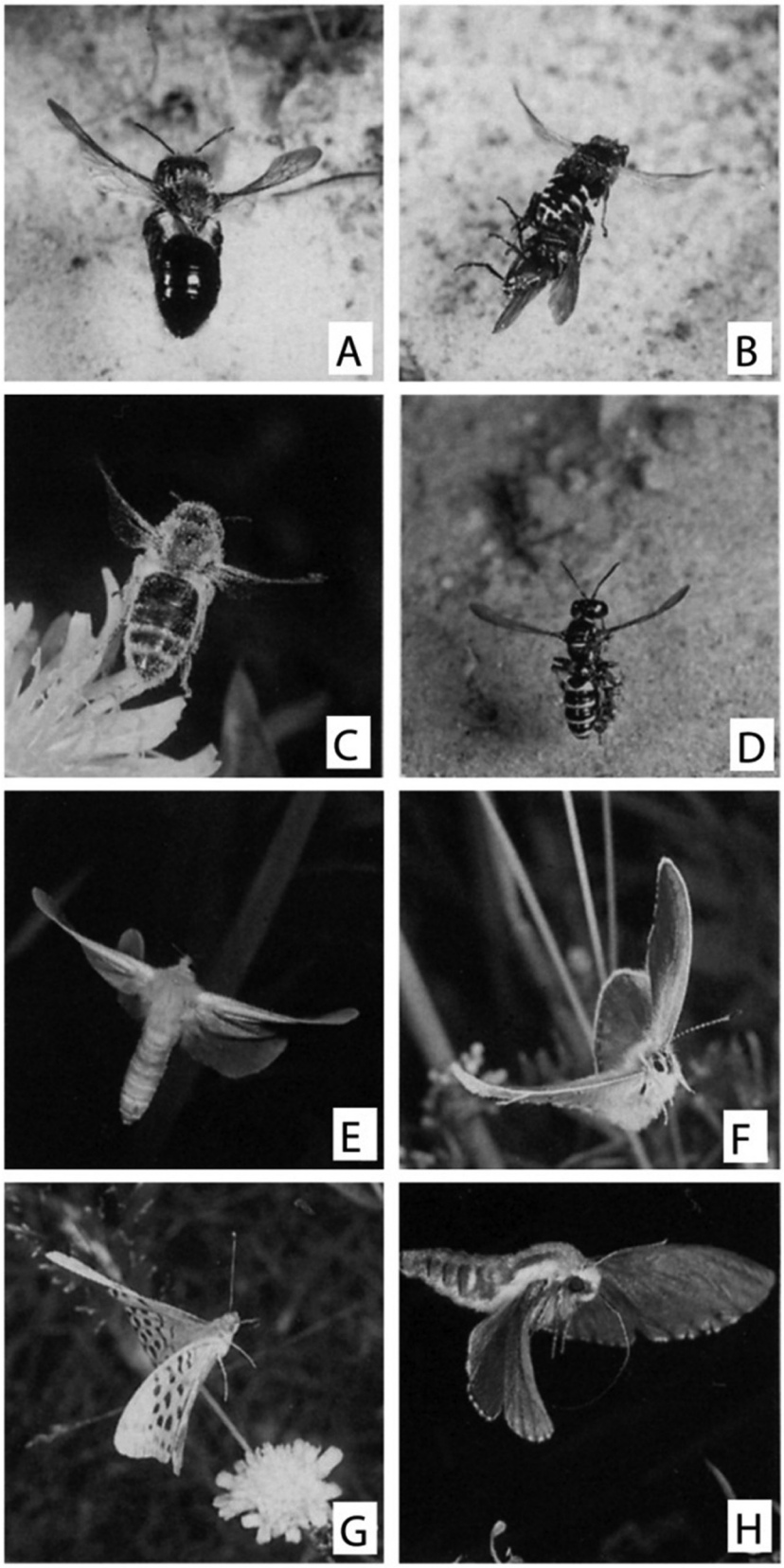

wings twist extensively and a torsional wave passes from the wing tip to the base at supination (e.g., Figs. 1C, 1E).

Beyond these general patterns, however, the degree to which insect wings deform during flight has not been well documented. Obtaining precise, fine-scale measurements of dynamic wing-shape changes occurring at high temporal frequencies presents numerous technical challenges. Thus, qualitative descriptions of wing bending based on still photographs (e.g., Figs. 1A–1H) tended to dominate the literature until recently. Beginning in the mid-1990s, fringe projection and related optical techniques in which deformations are measured via changes in light patterns projected onto flapping wings produced the first quantitative measurements of wing twisting and bending in dragonflies (Zeng et al. 1996; Song et al. 2001; Wang et al. 2003), bees (Zeng et al. 2000), and moths (Sunada et al. 2002*a*), although spatial resolution was limited by the projected optical pattern. Advances in the spatial and temporal resolution of high-speed video cameras coupled with improved photogrammetric techniques (Walker et al. 2009*b*) have resulted in high-resolution measurements of wing deformations in locusts and hover flies (Walker et al. 2009*a*, 2010).

High-resolution measurements show that insect wings undergo significant dynamic camber changes during flight, displaying instantaneous camber of up to 10% of chord length in locusts and up to 12% in hover flies (Walker et al. 2009*b*). In addition, many insect wings display significant dynamic twisting during flight of up to 25° in hawkmoths, 30° in locusts, and >50° in hover flies (Willmott and Ellington 1997; Walker et al. 2009*b*), as well as rapid torsional waves during stroke reversal (Mountcastle and Daniel 2009).

Wing materials and structure

Complex, three-dimensional wing deformations are controlled primarily by the structure of the wing, which simultaneously acts as a lever (transmitting forces from muscles at the wing base to the air), oscillating airfoil (accelerating air to generate and transmit aerodynamic forces to the body), and cantilevered beam (accepting changing patterns of bending and twisting forces without failure; Wootton, 1992). While it could be argued that their flexibility is an inevitable consequence of the properties of biological materials and the need to minimize wing mass and inertial costs, it is becoming increasingly clear that flexibility and controlled deformations are both beneficial and necessary to many aspects of wing functioning. Thus, an increasing number of studies have focused on the material properties, structure, and mechanical behavior of insect wings that underlie these deformations.

Insect wings are composed primarily of cuticle, a multilayered material consisting of chitin microfibers embedded in a protein matrix. The cuticle is arranged into tubular supporting veins and thin deformable membranes. Cuticle stiffness (E, Young's modulus) can vary from 1 kPa to 20 GPa, depending on hydration, sclerotization (the stiffening process that occurs after insects molt), and chitin-fiber orientation (Vincent and Wegst 2004).

Membrane thickness ranges from <0.5 μm in small thin wings to >1 mm in the protective forewings of beetles (Wootton 1992), and can vary widely within an individual wing (Rees 1975; Smith et al. 2000; Song et al. 2004). Directly measuring the Young's modulus of wing membranes is challenging, because thin, inextensible, heterogeneous structures do not lend themselves well to typical material-testing techniques; however, a handful of studies using nanoindentation (Song et al. 2004, 2007) or custom, miniaturized tensile testing (Smith et al. 2000), or static bending (Jin et al. 2009) techniques have provided relatively consistent measurements. These studies suggest that the Young's modulus of insect wing membranes is typically in the range of approximately 1.5–5 GPa, although this property can be anisotropic, and can vary widely throughout a wing (Jin et al. 2009; Smith et al. 2000). Several studies suggest that wing membranes may function as a stressed skin when enclosed by supporting veins, contributing to flexural rigidity rather than acting as a purely deformable element (Newman and Wootton 1986; Kesel et al. 1998; Wootton et al. 2000).

Wing veins are typically hollow tubes, with the main longitudinal veins (running from the wing base to the tip or trailing edge) transmitting fluid, oxygen, and sensory information (via nerves). There is currently no evidence to suggest that these fluid-filled veins are highly pressurized or that fluid pressure plays a significant role in the mechanical behavior of insect wings. Veins can be thin- or thick-walled and can have round, elliptical, or bell-shaped cross sections, which affects their bending stiffness along particular axes (Wootton et al. 2000). Cross veins connecting the longitudinal veins are typically filled with air and serve diverse structural roles, acting as strengthening brackets in some regions of the wing and promoting bending in others (Wootton et al. 2000).

Insect wing venation is generally denser near the wing base and leading edge, and vein diameter and cuticular thickness taper from base to tip. This arrangement reflects the distribution of bending stresses in flapping wings (Ennos 1989), providing additional strength where bending stresses are highest, and reducing mass towards the wing tips to minimize inertial power requirements. Beyond these general trends, venation pattern varies widely between groups of insects (Figs. 2A–2E). Surprisingly, these large differences in venation pattern do not significantly affect average bending stiffness (flexural stiffness, or EI) in the spanwise or chordwise direction (base to tip or leading edge to trailing edge). Rather, a strong scaling relationship suggests that average stiffness is related primarily to wing size (Combes and Daniel 2003*a*). Venation pattern is, however, likely to affect regional variation in stiffness. Measurements of spatial patterns of flexural stiffness in hawkmoth, dragonfly, and fly wings show that stiffness declines exponentially from wing base to tip (as well as from leading edge to trailing edge in hawkmoths and dragonflies), although details of the stiffness patterns differ (Combes and Daniel 2003*b*; Lehmann et al. 2011).

Many insect wings contain flexion and (or) fold lines, bands of flexible cuticle that run along wing membranes and often interrupt supporting veins to promote bending or folding along certain axes of the wing. These lines can function as two-way joints or as one-way hinges that prevent bending in one direction while promoting it in the other. Many wings contain one to three flexion lines that run longitudinally or radially, facilitating chordwise bending and twisting (Wootton 1979), and wings may also contain transverse flexion lines (from the leading edge to the trailing edge), which function as one-way hinges to promote ventral bending at the end of the downstroke. Some wings possess creases that do not normally bend during flight, but which prevent damage by crumpling reversibly during collisions (Mountcastle and Combes 2014).

Resilin, a flexible, highly elastic protein, has been found in the fold lines of some beetles and earwigs, potentially assisting in folding the wings when at rest, preventing material damage, and (or) contributing to elastic energy storage and wing deformations during flight (Haas et al. 2000*a*, 2000*b*). Resilin has also been found in the intersections between supporting veins in odonates (Figs. 3A–3C) (Gorb 1999; Donoughe et al. 2011), dipterans (Lehmann et al. 2011), and hymenopterans (Mountcastle and Combes 2013, 2014), insects that do not fold their wings at rest, suggesting a flight-related function for resilin. Experimental manipulations show that despite their small size, these resilin-filled joints contribute significantly to bending patterns and overall wing flexibility (Donoughe et al. 2011; Mountcastle and Combes 2014), due to the fact that the elastic modulus is typically at least three orders of magnitude lower than the surrounding cuticle (Vincent and Wegst 2004).

The mass distribution of wings has not been studied extensively, although it is likely to have a significant effect on wing deformations, particularly those caused by inertial forces. The mass of insect wings generally tapers from wing base to tip (Ennos 1989), but some

Fig. 2. Venation patterns in insect forewings: (A) dragonfly and damselfly (Odonata); (B) termite (Isoptera) and lacewing (Neuroptera); (C) wasp and bumblebee (Hymenoptera); (D) crane fly and hover fly (Diptera); (E) hawkmoth and butterfly (Lepidoptera). Images courtesy and reproduced with permission of S.A. Combes.

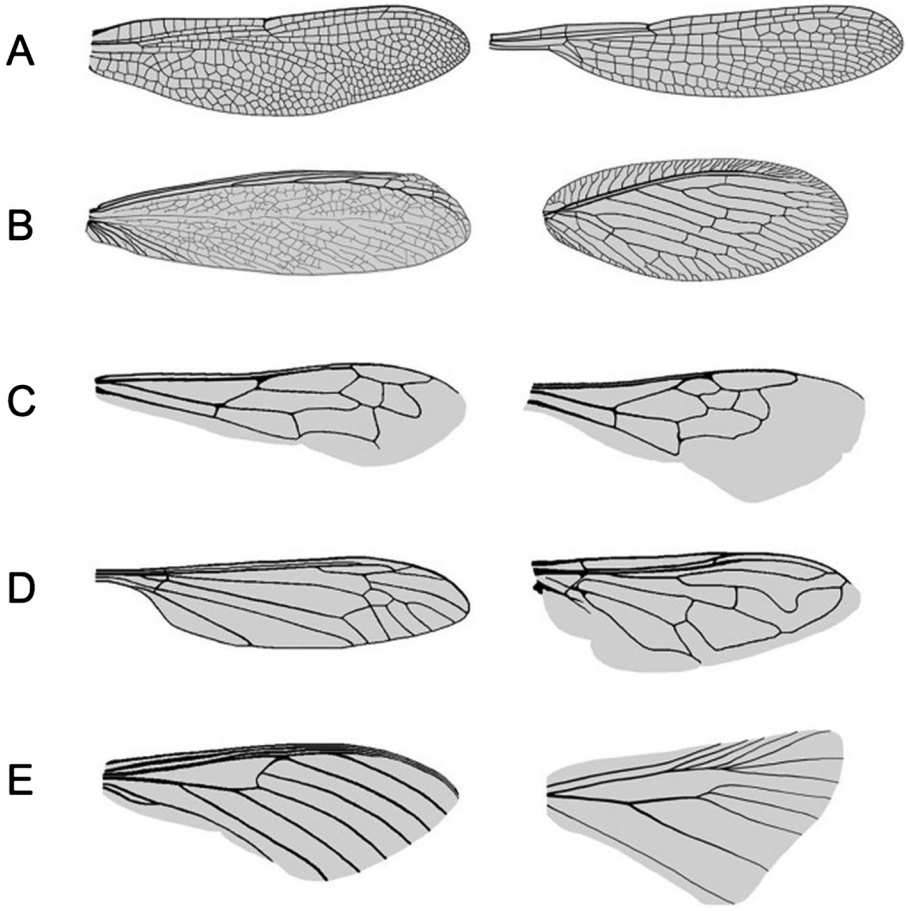

Fig. 3. Location and morphology of chordwise, resilin-containing joints in a damselfly wing: (A) damselfly wing with locations of flexible, resilin-containing chordwise joints indicated by black circles; (B, C) scanning electron micrographs of a resilin-containing joint with spikes that may prevent excessive bending. Images courtesy and reproduced with permission of J.D. Crall and S. Donoughe.

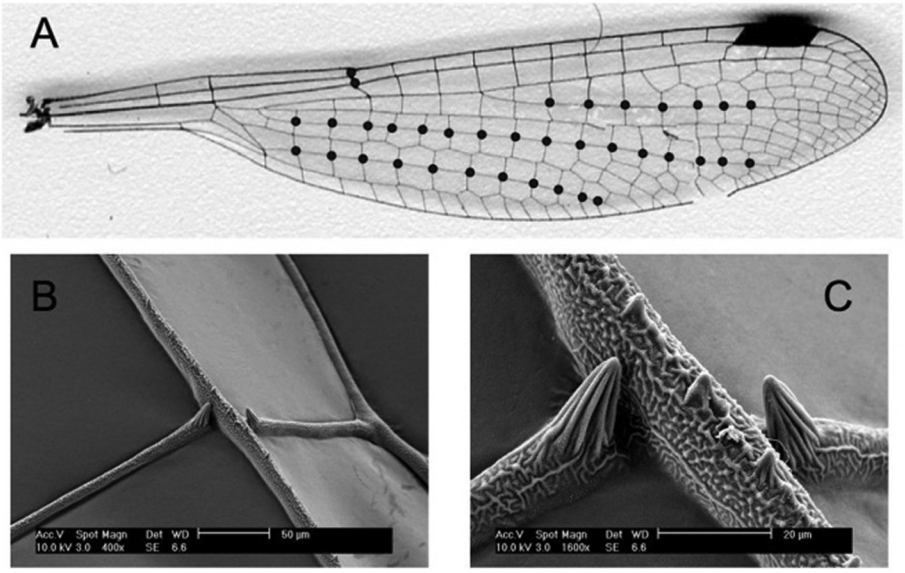

groups such as dragonflies and bees contain a pterostigma, a pigmented spot with greater mass than the surrounding cuticle, approximately 5%–10% total wing mass in dragonflies (Norberg 1972), located on the distal leading edge (Fig. 3A). Adding mass near the leading edge helps balance the chordwise distribution of mass (which is otherwise centered behind the torsional axis of the wing), potentially helping to regulate wing pitch and prevent flutter during gliding (Norberg 1972), and increasing wing-tip amplitude and upstroke–downstroke asymmetry during flapping flight (Chi et al. 2012).

Finally, the three-dimensional structure (e.g., corrugation or camber) of wings is likely to have a substantial effect on their mechanical behavior. Dragonflies are well known for extensive spanwise wing corrugation, but this corrugation is actually seen in many insect wings to some extent, especially near the basal leading edge (Rees 1975). Wing corrugation clearly provides structural benefits, increasing spanwise bending stiffness (Rees 1975) while minimizing material expenditure (Kesel et al. 1998) and allowing wings to twist extensively during flight (Sunada et al. 1998). Similarly, the wings of many insects exhibit some degree of camber at rest, particularly near the base, with a convex upper surface and concave lower surface (Wootton 1993). Cambered plates twist and bend more easily when pushed on their convex surface than on their concave surface (Ennos 1995); thus, camber may contribute to observed dorsal–ventral asymmetries in wing bending behavior and twisting behavior (Wootton et al. 2000; Combes and Daniel 2003*b*), as well as to the pronounced ventral flexion that occurs in many insect wings during supination (Figs. 1A–1H) (Wootton 1992).

Although aerodynamic force generation is likely the primary function driving many of these material and structural features, the design of insect wings may also reflect trade-offs or specialization for other aspects of flight performance, such as efficiency, versatility, maneuverability, or stability. In addition, insect wings must function over an extremely long lifespan, flapping millions of times in many cases, and must endure collisions without experiencing structural failure. Irreversible wing damage (particularly loss of area near the tips or trailing edges) accumulates over time in many insects and has been shown to reduce maximal force production and predation success in dragonflies (Combes et al. 2010), necessitate active neuromuscular control in hawkmoths (Fernández et al. 2012), and increase mortality in bumblebees (Cartar 1992) and honeybees (Dukas and Dukas 2011). In some insects, this damage is caused by collisions with vegetation (Foster and Cartar 2011) or other objects in the environment. Wings tend to deform readily and reversibly during collisions, due to either their overall structure (e.g., wing corrugation) (Newman and Wootton 1986) or morphological features such as flexion and fold lines (Mountcastle and Combes 2014).

Insect flight-muscle physiology

Insect flight is powered by muscle, which provides the force and mechanical power necessary to keep a dense flying animal aloft in a diffuse fluid. Insects typically have a large suite of flight muscles, very large ones responsible for producing the power required to fly and other smaller muscles responsible for fine-tuning the wing kinematics and providing control (Pringle 1957). The large flight power muscles (with the notable exception of dragonflies and their kin (Odonata)) are indirectly attached to the wings via the thorax, with one bilateral pair powering the downstroke and a second bilateral pair powering the upstroke. The flight power muscles may also be classified as synchronous or asynchronous. Synchronous muscles are controlled similarly to vertebrate skeletal muscle, with a discrete neural activation event for each muscle contractile event. Asynchronous or stretch-activated insect flight muscle requires only an occasional neural stimulus; contractions also result from stretching of the muscle and permit an oscillatory stretch–shorten cycle between the antagonistic upstroke and downstroke flight power muscles (Pringle 1949). Asynchronous muscle has evolved several times among insects (Dudley 2000) and evidence is mounting to support the hypothesis that asynchronous muscle provides more efficient production of mechanical power at high flapping frequencies than synchronous muscle. Production of aerodynamic forces via flapping wings requires the expenditure of mechanical power. Thus, the questions "how much power can flight muscle provide?" and "how efficient are muscles at converting chemical energy to mechanical work?" are central to linking insect flight muscle to the whole of insect physiology.

A variety of approaches have been used to understand muscle power and efficiency, although none have provided a direct measurement of the muscle and energetic performance of a freely flying insect. The work-loop technique (Machin and Pringle 1960) popularized by Josephson (1985) has now been widely applied to preparations ranging from nearly intact animals (e.g., Tu and Daniel 2004) to isolated muscle fascicles (e.g., Askew et al. 2010), and allows direct measurement of muscle mechanical power production for a given temperature, stretch, strain, and neural stimulus profile. Careful simultaneous measurement of heat production, CO_2 production, or O_2 consumption during work-loop experiments provides efficiency estimates. Comparison of work-loop results for maximum muscle power output and muscle efficiency (Josephson et al. 2000*b*; Josephson et al. 2001) from different insect species supports the hypothesis that asynchronous flight muscle provides greater power output, greater efficiency, and a higher operating frequency than synchronous muscle. The means by which asynchronous muscle achieves these benefits has been the focus of much experimental work, recently aided by the application of synchrotron imaging, which allows for the high-speed X-ray diffraction recording phase to be locked to the flapping frequency of a tethered insect (Fig. 4) and for recording diffraction patterns over time intervals of <1 ms (Dickinson et al. 2005; Irving 2006; Iwamoto et al. 2010; George et al. 2013; Walker et al. 2014).

In vivo X-ray diffraction of insect flight muscle

The greatest advances in experimental technique applied to the study of insect flight muscle have come from use of synchrotron radiation sources to provide in vivo X-ray diffraction recordings of the genus *Drosophila* Fallén, 1823 (Irving 2006) and bumblebees (Iwamoto et al. 2010) (Fig. 4). X-ray diffraction provides information on the molecular structure of the flight muscle at discrete instants within the contractile cycle. These measurements were first used to show that the spacing of the myofilament lattice does not change during a contraction cycle, although the volume occupied by the lattice does change slightly (Irving and Maughan 2000). Later synchrotron experiments with more accurate synchronization of the flapping cycle and synchrotron imaging suggest that strains in the thick filaments of lengthening muscle may store elastic energy, helping to overcome the inertial costs of flapping wings (Dickinson et al. 2005). These results also hint that cross-bridge attachment during lengthening is critical to stretch activation, a possibility explored in more detail in a later synchrotron study of bumblebee flight-muscle stretch activation (Iwamoto et al. 2010). Results from this work demonstrate that stretch activation could be regulated by mechanically triggered movement of tropomyosin, which was observed to change configuration quickly enough to support such a relationship at the 170 Hz flapping frequency used by the bumblebees. Together with additional classical discrete and skinned fiber experiments (Linari et al. 2004), these findings have produced an emerging consensus on the mechanisms underlying stretch activation in insect flight muscle.

Stretch activation of asynchronous insect flight muscle

Stretch activation reduces the energetic cost of muscle contraction by reducing the amount of calcium ions (Ca^{2+}) that must be

Fig. 4. Schematic of the synchrotron X-ray apparatus used for in vivo time-resolved X-ray diffraction of flight muscles of the fruit fly *Drosophila melanogaster*. The dorsolongitudinal (DLM), dorsoventral (DVM), and thoracic (TDT) muscles are shown in schematic form on the left. (Adapted from Irving and Maughan 2000; reproduced with permission of Biophys. J., vol. 78, issue 5, ©2000 Elsevier Science Ltd.)

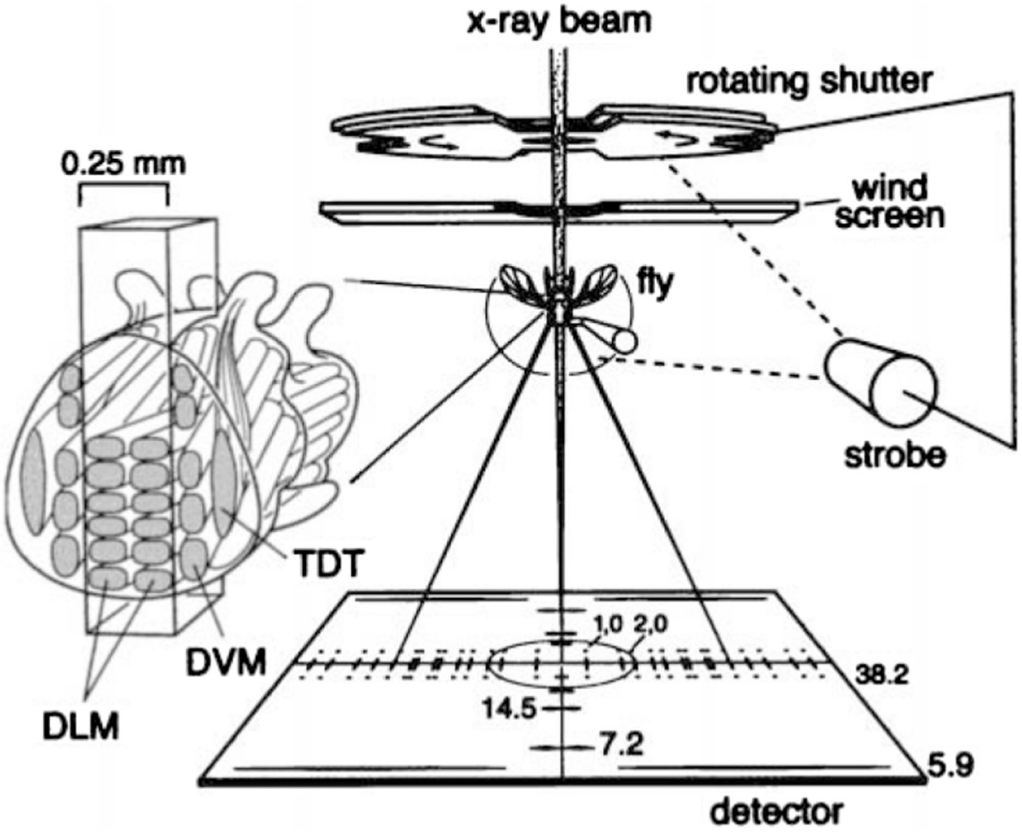

cycled in and out of the muscle sarcomere during each contraction. This increases the density of contractile elements and mass-specific mechanical power output of the muscle by replacing Ca^{2+} control elements with additional contractile elements (Josephson et al. 2000*a*). Given a threshold level of Ca^{2+} in the muscle, stretch activation allows continuous oscillatory work cycles at high frequency. Mounting evidence shows that Ca^{2+} activation and stretch activation engage the same fundamental pathway regulating myosin cross-bridge attachment (Linari et al. 2004). Work on isolated insect flight-muscle fibers has shown that Ca^{2+} and stretch activation are complementary; they do not inhibit one another but are also not additive. However, a certain fraction of cross bridges must be active for stretch activation to occur. This suggests that the sensor or trigger for stretch activation may be the cross bridge itself and that distortion of stretched, bound cross bridges displaces the muscle regulatory protein tropomyosin, exposing other myosin binding sites on the actin filament and allowing further cross-bridge attachment (Bullard et al. 1988; Agianian et al. 2004). Additional experiments on isolated indirect flight-muscle fibers from the giant waterbug genus *Lethocerus* Mayr, 1853 stimulated in a synchrotron X-ray diffraction recording system have further clarified the mechanical linkage implied by earlier experiments (Perz-Edwards et al. 2011). The mechanism appears to lie in the "troponin bridges", similar to actin–myosin cross bridges but connecting the myosin molecules in the thick filament to troponin in the thin filament. These troponin bridges pull tropomyosin aside during contraction, allowing further actin–myosin binding and providing a mechanical linkage underlying stretch activation in asynchronous insect flight muscle.

Aerodynamics of insect flight

Aerodynamic theory

Review of basic aerodynamics

Scale has a significant effect on the behavior of fluid flow and this makes the direct application of aircraft aerodynamic theory to insect flight problematic (Cloupeau et al. 1979; Zanker and Gotz 1990; Ellington 1995). A dimensionless number known as Reynolds number (*Re*) is often used to quantify scale, predict the behavior of the flow, and determine the most appropriate mathematical theory. *Re* quantifies the relative effect of inertial to viscous forces in a fluid flow and is given as

$$(1) \qquad Re = \frac{\rho l U}{\mu} = \frac{l U}{\upsilon}$$

where ρ is the density of the fluid, μ is the dynamic viscosity of the fluid, υ is the kinematic viscosity of the fluid, l is a characteristic length, and U is a characteristic velocity. In this case, l may be considered the chord length of the wing and U may be considered the velocity of the wing tip relative to the fluid. For insects, *Re* can range from <10 to 1000s, as shown in Fig. 5.

As an insect wing moves through air, forces are produced both in the direction of the motion of the wing and perpendicular to that motion. Drag is the force acting on the wing in the direction of its motion. This force can be broken down into two elements: pressure drag and skin friction. Pressure drag can be calculated from the pressure distribution around the wing and varies with the square of velocity. Skin friction is due directly to the air's resistance to shearing near the wing surface. This component of

Fig. 5. Forward velocity (V) as a function of Reynolds number (*Re*) (from Nachtigall 1981; reproduced with permission of Biophys. Struct. Mech., vol. 8, issues 1–2, ©1981 Springer Science+Business Media). Ranges of *Re* for unicellular organisms, microscopic organisms, small insects with bristled wings, larger insects with solid wings, birds, and large cetaceans are shown by the black boxes. The majority of insects fly at *Re* significantly larger than one where inertia dominates. The smallest insects are thought to fly at *Re* between 5 and 10; viscous effects are non-negligible.

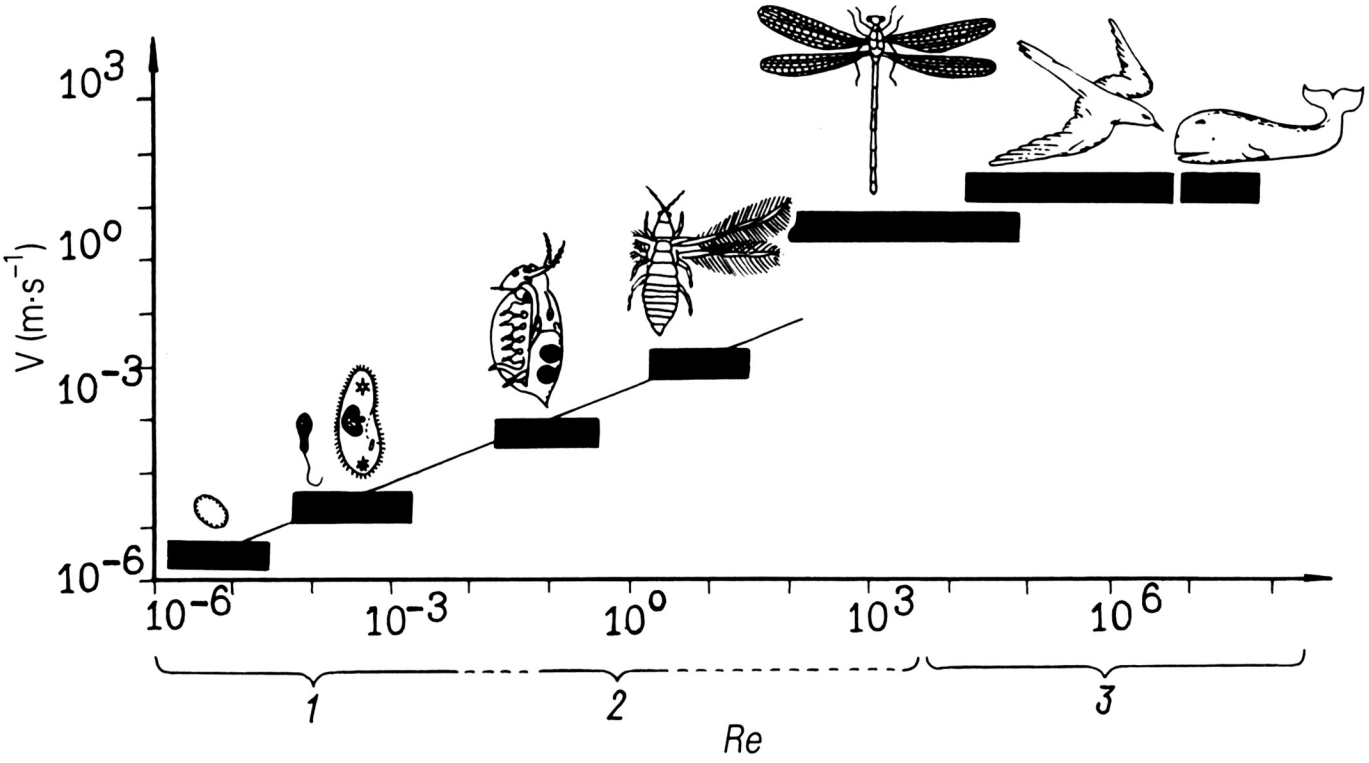

drag is proportional to the viscosity of air and the velocity. For most studies of insect flight, the pressure drag dominates and the drag acting on the wing is proportional to the square of the velocity. Lift can be considered any force that acts in the direction perpendicular to the motion of the wing. For an idealized airfoil in an inviscid fluid, lift is proportional to the circulation around the wing (Milne-Thomson 1966; Acheson 1990). Drag-based mechanisms may also contribute to lift when lift is defined in the direction acting against gravity (Wang 2004). More details on lift will be provided in the sections below.

A convenient way to compare lift and drag across insects and other animals is to define dimensionless lift and drag coefficients. These numbers depend upon the shape of the wing, *Re*, and the angle of attack (Vogel 1967; Dickinson and Gotz 1993). The angle of attack is the angle of the wing relative to the direction of motion. For a wing translating horizontally, the lift coefficient is maximized at about a 45° angle of attack and drag is maximized at a 90° angle of attack. For *Re* >>1 that are characteristic of insect flight, the lift and drag coefficients are given as

$$C_L = \frac{2F_L}{\rho S U^2} \quad (2)$$

$$C_D = \frac{2F_D}{\rho S U^2} \quad (3)$$

where C_L is the lift coefficient, C_D is the drag coefficient, S is the surface area of the wing, F_D is the drag acting on the wing, and F_L is the lift. For *Re* <<1, lift is negligible and drag scales as $\mu l U$. For intermediate *Re*, forces on the wing scale as some combination of the high and low *Re* approximations.

Two conventions for lift and drag have been used in the insect flight literature. As described above, lift may be defined as the component of the force acting perpendicular to the motion and drag may be defined as the force acting in the direction of motion. If the wing flaps in a horizontal plane, then the lift is equivalent to the vertical force, F_v, and drag is equivalent to the horizontal force, F_h (see Fig. 6A). If the motion of the wing is not horizontal, then the direction of lift is no longer vertical and the direction of drag is no longer horizontal (see Fig. 6B). To describe lift as the force acting against gravity, lift and drag are sometimes set to the vertical and horizontal components of the force, respectively. This also avoids some complications in interpreting the direction of motion for rotating wings. In this review, the conventions given in Figs. 6A and 6B will be used.

The vast majority of work on the aerodynamics of insect flight has been performed on animals engaged in hovering flight, which is the most experimentally tractable behavior for making precise measurements of wing movements and also the most energetically challenging flight mode. Thus, this review also focuses on hovering flight aerodynamics.

Unsteady aerodynamics and the leading-edge vortex

Several unsteady aerodynamic mechanisms specific to flapping flight can augment the total lift generated. One such mechanism is wing rotation, whereby the angle of attack changes over time. The wings substantially rotate at the end of the upstrokes and downstrokes, providing the wing with a positive angle of attack and generating additional rotational circulation about the leading edge of the wing (Sane and Dickinson 2002). This rotational circulation is proportional to the angular velocity of rotation and results in an additional force upwards. Wake capture and other vortex effects from previous strokes have also been shown to enhance lift

Fig. 6. Definitions of lift and drag for idealized hovering along a horizontal stroke plane (A) and along an inclined stroke plane (B) (adapted from Wang 2004; reproduced with permission of J. Exp. Biol., vol. 207, issue 23, ©2004 The Company of Biologists Ltd.). In this diagram, lift is defined as the force acting perpendicular to the direction of wing motion and drag is defined as the component of the force acting in the direction of wing motion. When the wing flaps along a horizontal plane, lift is equivalent to the vertical force (F_v) and drag is equivalent to the horizontal component of the force (F_h). When the wing flaps along an inclined plane, the direction of lift is no longer vertical and the direction of drag is no longer horizontal.

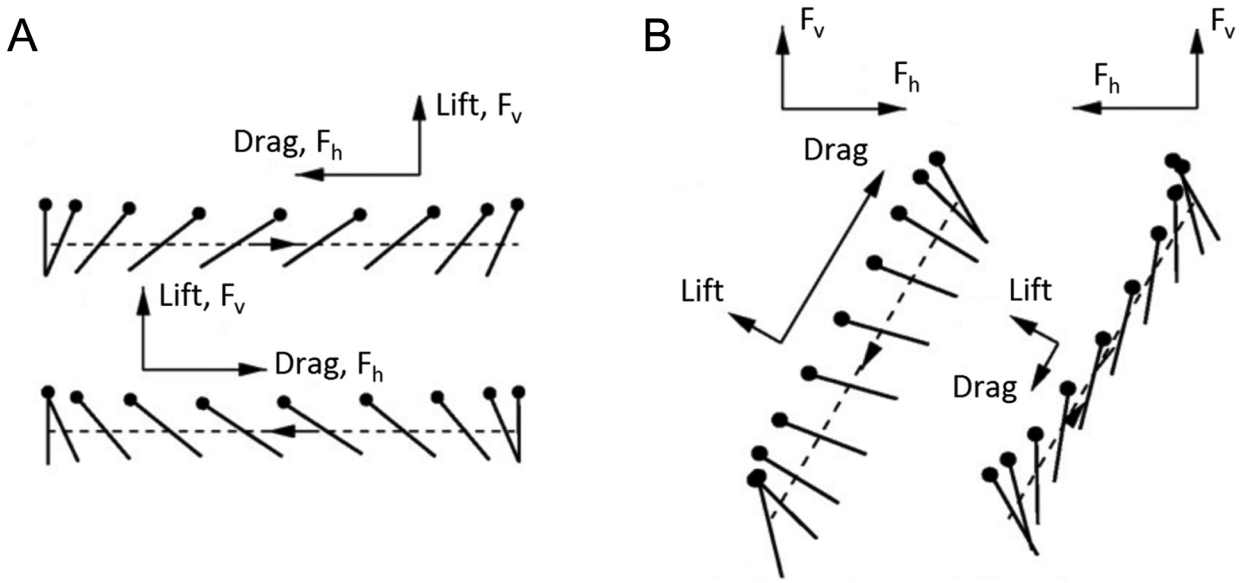

generation in flying insects (Dickinson et al. 1999; Wang 2000; Sane and Dickinson 2002). The basic idea is that the velocity of the wing relative to the background flow can be higher as the wing translates through its own wake. This increased velocity of the wing relative to the nearby flow results in higher forces.

Another aerodynamic mechanism that has received much attention over the past decade is the formation of a stable, attached leading-edge vortex (LEV) (Ellington et al. 1996; Dickinson et al. 1999; Srygley and Thomas 2002; Bomphrey et al. 2006; Lentink and Dickinson 2009; Chen et al. 2010; Yilmaz and Rockwell 2011). The flapping motion of the wings during each stroke results in the separation of flow at the sharp leading edge and the formation of the LEV over the top surface of each wing (see Figs. 7A, 7B). The presence of the attached LEV increases the lift produced through a beneficial alteration of the streamwise pressure gradient. This gradient increases both the steady state and the instantaneous circulation over the wing and maintains the negative pressure region in the wake of the wing. For an airplane wing in pure translation, stall occurs above some critical angle of attack when the LEV separates from the wing and lift consequently drops. Stall, however, is suppressed for insects flying at high angles of attack and this allows for large lift forces.

To understand the mechanism of the formation of the LEV, consider a wing revolving from rest that is immersed in a viscous fluid. At the onset of motion, the fluid is sheared because the wing has a nonzero tangential velocity relative to the surrounding fluid. This discontinuity creates a sheet of concentrated vorticity. At later times, the vortex sheet is transported away from the wing by diffusion and convection. The vortex sheet "rolls up" as a result of the negative pressure region generated instantaneously behind the wing due to its motion. The rolled vortex sheet forms the LEV and its presence maintains the negative pressure region behind the wing that leads to higher lift forces. Numerous experimental and numerical studies have shown that the LEV does not separate at high angles of attack for *Re* relevant to insect flight (Maxworthy 1979; Ellington et al. 1996; Van den Berg and Ellington 1997; Usherwood and Ellington 2002; Birch et al. 2004; Maxworthy 2007; Lentink and Dickinson 2009). As a result, insects can fly at high angles of attack where large lift forces are generated.

The LEV does not typically separate from the wing until wing reversal; this observation has inspired a large body of work to understand the stability (or instability) of the LEV (Birch and Dickinson 2001; Thomas et al. 2004; Lentink and Dickinson 2009; Bomphrey et al. 2010). It is well known that translating plates at high angles of attack generate a wake of alternating shed vortices known as the von Karman vortex street (Batchelor 1967). A fundamental question in insect flight aerodynamics is then to ask, "why does the LEV not separate during the stroke for similar angles of attack?" Wang et al. (2004) used two-dimensional simulations and physical models to show that one of the most significant differences between two-dimensional and three-dimensional flight is the stability of the LEV after three chord lengths of travel. If the wing does not translate farther than three chord lengths, then two-dimensional simulations accurately describe the behavior of the LEV because separation does not occur before reversal. Studies focusing on the wakes of live insects have considered variations in structure and stability of the LEV due to forward flight, angle of attack, and wing design and their consequences to aerodynamic performance (Srygley and Thomas 2002; Bomphrey et al. 2006, 2012; Young et al. 2009).

In some cases, separation may be suppressed due to spanwise flow and vortex stretching along the LEV, particularly in situations dominated by rotation. Although there is little rigorous mathematical theory regarding the stability of the attached LEV, insight can be gained by considering a three-dimensional wing with an attached LEV rotating about its base. There are three processes occurring in this case: the convection of the vortex, the intensification of vorticity when vortex lines are stretched, and the diffusion of vorticity by viscosity (see Acheson 1990). In order for the LEV to remain stably attached to the wing, these three processes should be balanced. It is well known that the rotational motion of the wing results in axial flow along the wing (Liu et al. 1998; Ellington 1999; Birch et al. 2004). The axial flow is a result of a spanwise pressure gradient and is inherently a three-dimensional

Fig. 7. Diagram of the leading edge vortex (LEV) on the wing of the fruit fly *Drosophila melanogaster* (A) and photo of the LEV visualized on a dynamically scaled model wing (B) (from Lentink et al. 2009; reproduced with permission of ©2009 Springer-Verlag). The LEV remains stably attached to the wing when it revolves but separates from the wing in pure translation. Figure 7A appears in colour on the Web.

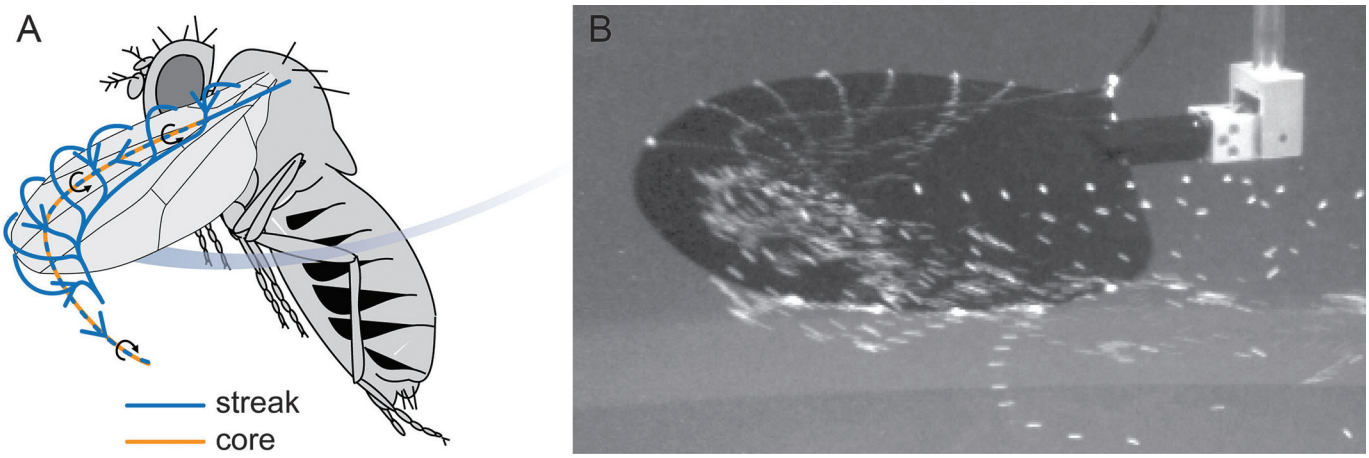

phenomenon. The LEV is stretched as a result of the axial flow and the three processes described above may be balanced so that the vortex is stable. Using flow visualization and force measurements on a dynamically scaled model wing, the LEV was found to be stabilized (and the aforementioned processes are balanced) by the "quasi-steady" centripetal and Coriolis accelerations resulting from the propeller-like sweep of the wing (Lentink and Dickinson 2009).

Quantifying flow fields around flying insects

Advances in high-speed flow visualization over the past decade have enabled scientists to resolve both planar two-dimensional and fully three-dimensional flow fields around flying insects (Bomphrey et al. 2012). One approach that has allowed researchers to obtain spatially and temporally resolved quantitative flow-field data is particle image velocimetry (PIV). PIV is a nonintrusive technique that can be used to obtain instantaneous flow velocities by recording and processing the single- or multiple-exposed images of tracer particles suspended in the fluid. The particle images are then processed using correlation-based techniques to construct the velocity vector field of the fluid flow (Willert and Gharib 1991; Adrian 2005). Two-dimensional planar PIV allows for the calculation of two-dimensional vector fields in a plane, while stereoscopic PIV permits the calculation of three-dimensional vector fields in a two-dimensional plane. For periodic flow fields with regular behavior, such as those obtained in tethered flight, data from a series of planes can be used to reconstruct the three-dimensional flow fields (Bomphrey et al. 2006; Lentink and Dickinson 2009). The development of tomographic PIV has enabled the reconstruction of complex three-dimensional wakes including non-periodic vortex wakes such as those seen in forward flying and maneuvering insects (Bomphrey et al. 2012). Tomographic PIV allows one to record and process a volume of tracer particles suspended in the fluid using several cameras to record simultaneous views of the illuminated volume (Elsinga et al. 2006).

The application of PIV to the wakes generated by flying insects has illuminated complex features of the leading-edge and trailing-edge vortices. Bomphrey et al. (2006) performed one of the first PIV studies on tethered hawkmoths to obtain two-dimensional slices of the vortex wake. They observed a strong LEV towards the end of the downstroke that corresponded to the maximum upward force generated during the stroke. They also found that the LEV extends continuously from wing tip to wing tip and across the thorax. Fuchiwaki et al. (2013) used PIV to reconstruct the LEV dynamics in the painted lady (*Cynthia cardui* (L., 1758) = *Vanessa cardui* (L., 1758)) and paper kite (*Idea leuconoe* Erichson, 1834) butterflies and also found that continuous vortex rings were formed and shed downstream at the end of each half stroke. Using smoke visualization, Bomphrey et al. (2010) showed that there are two separate LEVs that are not connected across the thorax in bumblebees. They also note that the LEV pair is less efficient than those in which left and right wings are aerodynamically linked.

Physical, numerical, and mathematical models

Recent progress in computation, flow visualization, and robotics has also enabled rapid advances in our understanding of insect flight and other forms of animal locomotion (Miller et al. 2012). Given the scale and frequency of flapping characteristic of many of the smallest flying insects, such as fruit flies and thrips, it is challenging to obtain detailed flow and force information of flight in a controlled manner. This difficulty led to the development of dynamically scaled physical models to resolve detailed characteristics of the flow fields (Ellington 1999; Birch and Dickinson 2003). Around the same time, advances in computing hardware and numerical methods made the simulation of moving boundaries in viscous fluids possible (Liu et al. 1998; Wang 2000; Peskin 2002; Mittal and Iaccarino 2005; Xu and Wang 2006). During the past decade, scientists have used computational fluid dynamics (CFD) to obtain spatially and temporally resolved flow fields and pressure distributions that would not always be easily obtained experimentally.

Dynamically scaled physical models

The use of robotic flappers to understand insect flight dates back to the pioneering work of Maxworthy (1979). Two of the more recent robotic insects used to study flight with sophisticated flapping kinematics include the "flapper" (Van den Berg and Ellington 1997) and the "robofly" (Dickinson et al. 1999). The flapper was used to mimic the flight of the hawkmoth and consisted of a body and two wings mounted on a stand. Smoke visualization produced one of the first detailed descriptions of the three-dimensional LEV. The robofly was used originally to investigate *Drosophila* flight. This model allowed for the measurement of vertical and horizontal forces as functions of time. Subsequent studies also used PIV to reveal the complex structure of the LEV and details of the wake in space and time (Birch et al. 2004; Lentink and Dickinson 2009) (see Figs. 8A–8C). Validation of full Navier–Stokes simulations (Zheng et al. 2013) and characterization of the LEV for accelerating rotating wings has recently been demonstrated using PIV (Elimelech et al. 2013). The results suggest that models using steady wing rotation are not adequate for predicting the performance of wings flapping at *Re* >1000.

Fig. 8. Diagram of the dynamically scaled robofly immersed in mineral oil from Dickinson et al. (1999; reproduced with permission of Science, vol. 284, issue 5422, ©1999 The American Association for the Advancement of Science) (A). Two axis force sensors are located at the base of each wing. Velocity fields around the model wings obtained from two-dimensional particle image velocimetry (PIV) for Reynolds numbers (*Re*) 10 (B) and 80 (C). The arrows show the direction of the flow, while the length of each arrow and the colour map show the magnitude of the velocity.

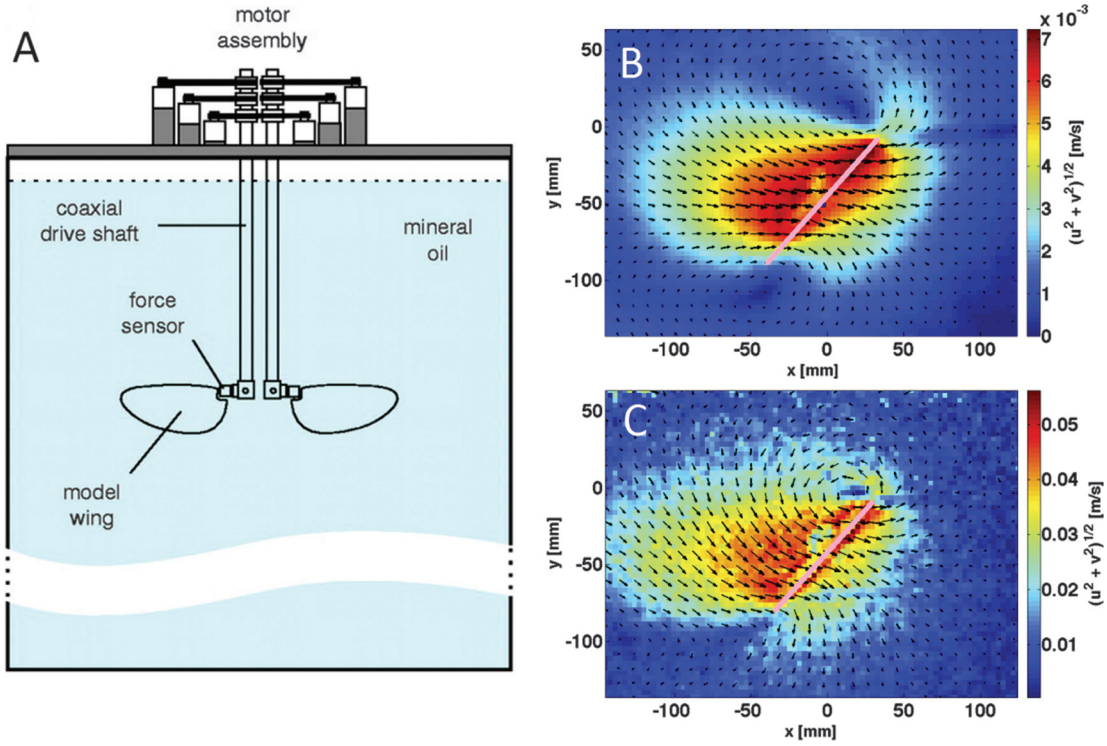

Modifications of the original robofly have also revealed new aerodynamic insights. Dickson and Dickinson (2004) considered forward-flight aerodynamics by translating the robofly while simultaneously flapping its wings. They were able to characterize the forces generated during simplified forward flight using a modified quasi-steady model that makes use of the ratio of the chordwise components of flow velocity at the wing tip due to translation and revolution. Dickson et al. (2010) later modified the robofly with a torque feedback mechanism to study the dynamics of yaw turns. The yaw torque produced by the wings was used to determine the rotation of the robofly; their results confirm that a first-order linear model with stroke-averaged force coefficients is sufficient to capture the yaw dynamics. By immersing the robofly in water and raising the *Re*, Altshuler et al. (2005) modeled honeybees. They determined that the relatively low stroke amplitude and high wingbeat frequency of honeybee flight generates relatively larger lift forces during stroke reversals than for fruit flies and other insects.

Over the past decade, other dynamically scaled robotic models have been developed and used to study fluid dynamical questions related to many species of insects (Lu and Shen 2008; Zheng et al. 2009) and other forms of animal locomotion (Vandenberghe et al. 2004; Tangorra et al. 2010; Jones and Babinsky 2011; Levy et al. 2011). Sunada et al. (2002*b*) constructed a dynamically scaled mechanical model of a thrips forewing that had a bristled design. The forces acting on the bristled wing were a little smaller than for a solid wing; a possible aerodynamic benefit for this wing design was not evident. Lu and Shen (2008) used an electromechanical model of a dragonfly wing immersed in water and measured the three-dimensional flow structures around the wing with phase-lock based multislice digital stereoscopic particle image velocimetry (DSPIV). At *Re* of about 1600, they found that the LEV system consists of a primary vortex and three minor vortices that are highly time-dependent in structure. Ishihara et al. (2009) used a dynamically scaled model of a crane fly wing that was able to bend about the leading edge. Their results suggest that a passive pitching motion of the wing can reproduce the kinematics of a crane fly's flapping wing. Phillips and Knowles (2013) designed an insect-like flapping wing at *Re* of approximately 15 000 and found that the LEV does not separate during the entire flapping half cycle.

Numerical models

Recent developments in CFD have made the simulation of moving structures immersed in two- or three-dimensional fluids possible (Hou et al. 2012). These advances have led to a wide variety of studies that apply computation to solve aerodynamic problems related to insect flight (Wang 2000; Sun and Lan 2004; Miller and Peskin 2009; Vanella et al. 2009). The fundamental challenge is the efficient and accurate handling of a moving boundary in a fluid. Although some commercial software packages are available, there is not a one-size-fits-all numerical method most appropriate for any given question.

One approach is to use conforming-mesh methods where the fluid equations are solved to determine the forces on the boundary, a structural computation is done to move the boundary, and a new fluid mesh is created (Newman Iii et al. 1999; Liu 2009). These approaches allow for high accuracy near the boundary but are typically computationally expensive. For simple cases such as a single wing, coordinate transformations and conformal mapping can be used to resolve the flow near the boundary and avoid grid regeneration (Wang 2000; Alben and Shelley 2005). Another approach is to solve the equations of fluid motion on a fixed Cartesian grid, define the wing on a moving Lagrangian grid, and develop a method to handle the interactions between the two grids without regenerating the fluid grid at each time step (Li and

Fig. 9. Vorticity fields generated from two-dimensional simulations during one period of an optimized wing motion (from Pesavento and Wang 2009; reproduced with permission of Phys. Rev. Lett., vol. 103, issue 11, ©2009 American Physical Society). The wing motion was selected to minimize aerodynamic power required for steady flight.

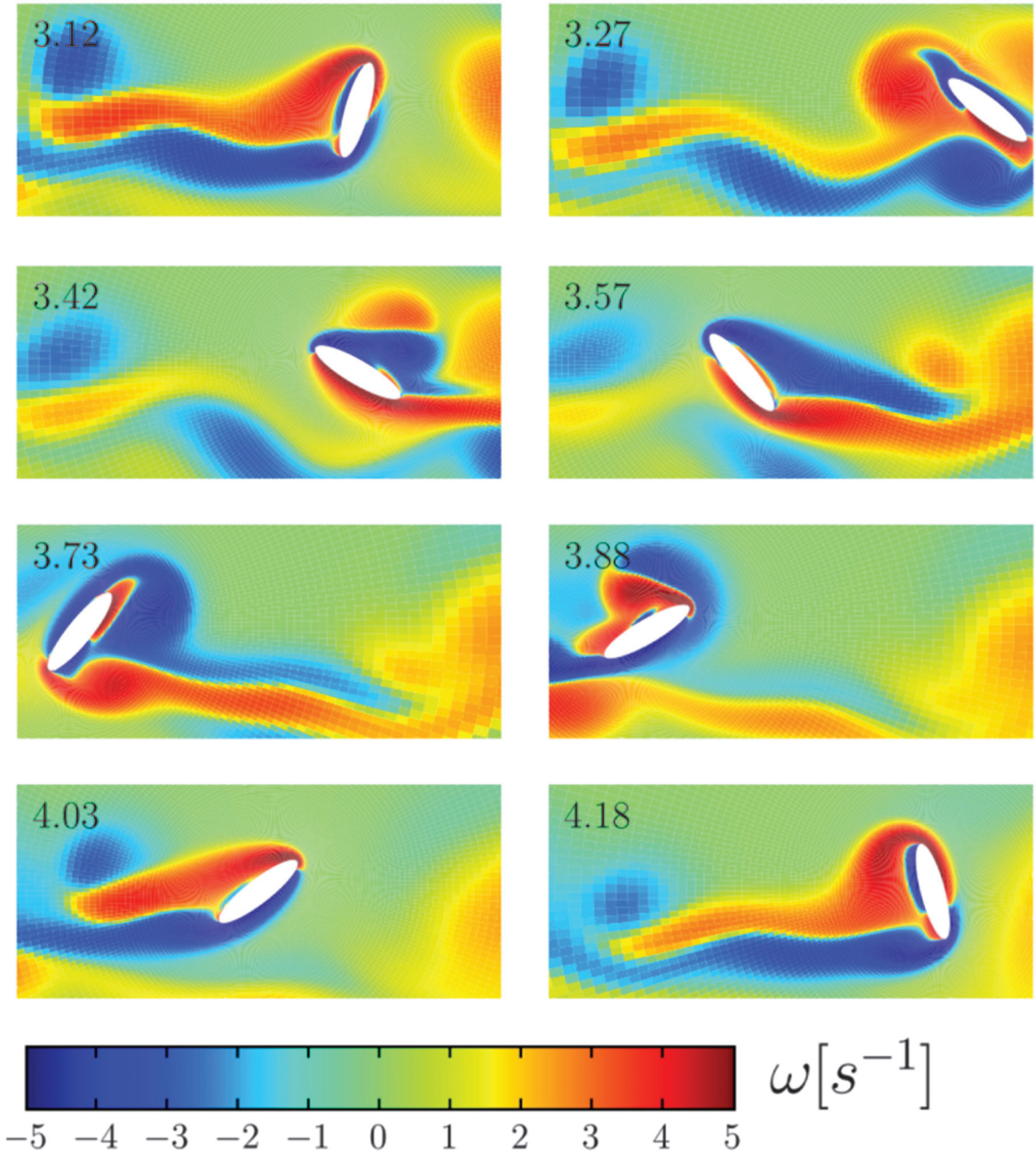

Lai 2001; Peskin 2002; Lee and LeVeque 2003; Mittal and Iaccarino 2005; Xu and Wang 2006; Bhalla et al. 2013; Wiens and Stockie 2015). In the cases of complex geometries or multiple wings, the immersed boundary method also allows one to solve moving boundary problems with relative ease (Peskin 2002; Mittal and Iaccarino 2005).

Two-dimensional simulations have allowed for large parameter sweeps, while three-dimensional simulations have elucidated complex details of the LEV and wake. Two-dimensional simulations of single flapping wings have shown that the lift to drag ratio generated during flight is lower for the smallest insects that fly at *Re* less than approximately 30 (Wang 2000; Sun and Tang 2002; Miller and Peskin 2004). Pesavento and Wang (2009) performed two-dimensional simulations to determine the minimal aerodynamic power needed to support a specified mass against gravity. Snapshots in time of the vortex wake behind the optimized wing stroke are shown in Fig. 9. Sun and Lan (2004) performed a three-dimensional simulation of a dragonfly (sedge darner, *Aeshna juncea* (L., 1758)) in hovering flight. Their results showed that the vertical force coefficient of the flapping wing is twice as large as the quasi-steady value. Three-dimensional simulations have also been used to quantify the LEV for hawkmoth wings (Nakata and Liu 2012*a*) and for *Drosophila* in free flight (Ramamurti and Sandberg 2007). Finally, Young et al. (2009) used three-dimensional CFD based on detailed wing kinematics to simulate the flight of the desert locust (*Schistocerca gregaria* (Forsskål, 1775)) and found that the wing topography and bending dynamics have significant aerodynamic consequences.

Fig. 10. Diagram of the clap-and-fling mechanism from Weis-Fogh (1973; reproduced with permission of J. Exp. Biol., vol. 59, issue 1, ©1973 The Company of Biologists Ltd.) and Sane (2003; reproduced with permission of J. Exp. Biol., vol. 206, ©2003 The Company of Biologists Ltd.). The wings clap together at the end of the upstroke (A–C), peel apart about the trailing edge at the beginning of the down stroke (D–F), and finally rotate apart (G–I). A downward jet is produced during the clap as the wings rotate together. During the fling, two large leading-edge vortices (LEV) form and no trailing-edge vortices form initially. This has the effect of increasing the lift generated. Figure appears in colour on the Web.

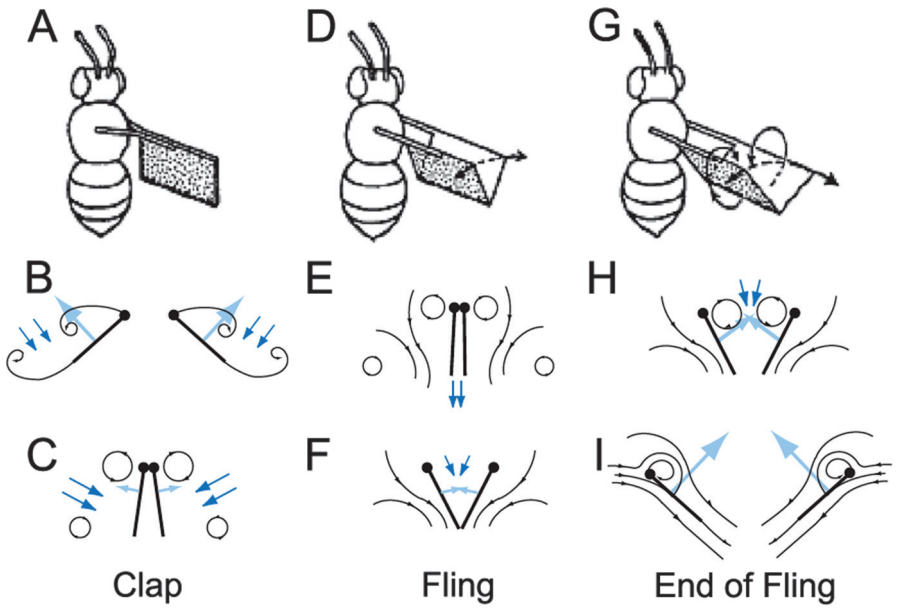

A current challenge in the field of CFD is to efficiently solve the fully coupled fluid–structure interaction (FSI) equations of a flexible wing that is deformed by the fluid in an unprescribed way due to the resulting fluid forces acting on the wing. The immersed boundary method offered one of the first ways to solve this fully coupled FSI problem (Peskin 1972); it has since been used to determine that flexibility can reduce the lift to drag ratio during clap and fling (Miller and Peskin 2009). On the other hand, immersed boundary methods on uniform grids encounter the difficulty in resolving fluid flow at the wing tips. This problem has motivated efforts to develop improved algorithms for addressing sharp-interface problems (Griffith and Peskin 2005; Xu and Wang 2006; Mittal et al. 2008). Another approach to FSI taken by Nakata and Liu (2012*a*, 2012*b*) was to use a loosely coupled finite element method based computational structural dynamic (CSD) model and a CFD model to simulate the flight of a hawkmoth with flexible wings. When the inviscid approximation is valid, numerical methods such as the vortex-sheet method (Krasny 1986, 1991) and vortexlets (Shukla and Eldredge 2007) can be used to solve the FSI problem much faster, enabling the exploration of large parameter spaces (Alben 2009; Mountcastle and Daniel 2009).

Wing–wing interaction

Aerodynamic studies using physical models and CFD suggest that wing–wing interactions are important for lift augmentation during flight. For some of the smallest flying insects, the LEV are strengthened when the wings are clapped together and then peeled apart at the beginning of the downstroke (Lighthill 1973; Weis-Fogh 1973; Maxworthy 1979). In the case of four-winged insects, the vortices shed off the forewings can either augment or reduce the vertical force produced depending upon the interactions between the vortex wake of the forewing and the motion of the hind wing (Wang and Russell 2007). The effects of both types of wing–wing interaction on thrust production, maneuverability, and stability warrant further investigation.

Clap and fling

Of the five published species of insects captured in flight with wingspans <1 mm, all of them clap their wings together at the end of each upstroke and fling them apart at the beginning of each downstroke (Miller and Peskin 2009). As a result of this motion, the LEV of one wing acts as the trailing-edge vortex of the other wing. Since these vortices are mirror images of each other, the circulation about the pair of wings and the total vorticity in the flow field are conserved (see Figs. 10A–10I). This is significant because both leading-edge and trailing-edge vortices are formed by single wings in pure translation and the formation of such symmetric vortex pairs results in smaller lift forces (Mao and Xin 2003; Miller and Peskin 2005). Kolomenskiy et al. (2011) used numerical simulations to show that the clap and fling mechanism is similar between two dimension and three dimension and across a wide range of *Re*. Srygley and Thomas (2002) used smoke visualization to show that two LEV form during two phases of acceleration during the downstroke: the initial fling and the subsequent acceleration once the wings have separated. Lehmann et al. (2005) showed using a dynamically scaled physical model that the lift-enhancing effects of the clap and fling mechanism are rapidly diminished as the initial gap between the wings widens. The magnitude of drag generated has received less attention in the literature, but it is known that very large forces are required to clap the wings together and to fling the wings apart when viscous forces are significant (Miller and Peskin 2009).

Wing-pair interactions

The aerodynamic benefits of forewing – hind wing interaction depend greatly upon the kinematics of the stroke. Thomas et al. (2004) used flow visualization in tethered and free-flying dragonflies to reveal the unsteady aerodynamic mechanisms employed by wing pairs. They found that dragonflies use counter-stroking kinematics in free flight. These wingbeat kinematics produced an attached LEV on the forewing during the downstroke, attached flow on the forewing during upstroke, and attached flow around

the hind wing throughout the cycle. Rival et al. (2011) used a two-dimensional tandem pitching and plunging configuration with similar dragonfly kinematics and found that only the tandem phasing of 90° generated levels of thrust similar to a reference single plate. This tandem configuration also generated more constant thrust over the entire wingbeat cycle. Using two-dimensional numerical simulations, Wang and Russell (2007) found that the out of phase motion used in steady hovering flight comes close to minimizing the power needed to generate sufficient vertical force to stay afloat. Usherwood and Lehmann (2008) noted that flying with two pairs of wing provides no obvious advantage in terms of lift. They did demonstrate, however, using a mechanical model dragonfly that two wing pairs can be highly effective at improving aerodynamic efficiency.

It is known that dragonflies switch to in-phase strokes during periods of sustained acceleration to reach speeds of up to 10 $m \cdot s^{-1}$ (Alexander 1984; May 1991). Thomas et al. (2004) used high-speed smoke visualization to show that this wing-beat pattern produces a single attached LEV across both wing pairs. The strong LEV structure across the forewings and hind wings generates the additional forces required for acceleration. Zheng et al. (2009) also noted that the in-phase mode used during acceleration enhances the lift on both wings.

For beetles, the elytra may also play a role in augmenting aerodynamic forces. Johansson et al. (2012) used three-dimensional PIV of the beetle's wake to show that the presence of the elytra increases vertical force production by approximately 40%.

Aerodynamic effects of wing flexibility and dynamic shape changes

Although *Re*-scaled physical models have been transformative in shaping our understanding of unsteady force generation mechanisms, they have provided little insight into the effects of wing flexibility on force generation. Studies of two-dimensional model wings accelerating from rest (Dickinson and Gotz 1993) or rotating three-dimensional model wings (Usherwood and Ellington 2002) suggest that static camber and twist have little effect on unsteady, translational force production. However, reproducing realistic dynamic shape changes in *Re*-scaled physical models is a challenging problem. No known scaling relationship exists that would allow one to scale wing flexibility to produce realistic passive deformations in response to inertial and aerodynamic loads. *Re*-scaled models employing flapping wings with a range of spatially uniform, isotropic Young's moduli (i.e., uniform flexibility) show that stiffer wings produce greater forces (Zhao et al. 2010).

In contrast to the physical modeling studies mentioned above, two-dimensional and three-dimensional numerical modeling studies suggest that wing flexibility enhances force production, efficiency, and other aspects of aerodynamic performance. Incorporating coupled FSI (and thus directly modeling passive wing deformations) is more feasible in two-dimensional simulations and this approach has produced several interesting results regarding wing flexibility. Flexible two-dimensional wings display higher force production, lift to drag ratios, and efficiency than rigid wings by enhancing wake capture during stroke reversal (Vanella et al. 2009); flexible wings produce less drag and in some cases more lift during clap and fling at low *Re* (Miller and Peskin 2009). In addition, flexible, oscillating two-dimensional wings display peaks in lift and thrust production that are highly sensitive to the distribution of flexural stiffness (Mountcastle and Daniel 2009). Most recently, a three-dimensional numerical study of a hawkmoth wing with passive wing deformations suggests that wing flexibility increases downwash in the wake and enhances force production by delaying LEV breakdown near the wing tip and improving wing-tip kinematics just before stroke reversal. The model also shows that passive wing twisting enhances hovering efficiency (Nakata and Liu 2012*a*).

Following the advances in photogrammetric techniques that led to high-resolution measurements of insect wing deformations during flight (Walker et al. 2009*b*), several groups performed three-dimensional CFD studies that explored the effects of passive wing deformations indirectly, by comparing the performance of model wings that accurately reproduced wing deformations to those with dynamic camber and (or) twist computationally removed. One study showed that wing flexibility improves force production and reduces power requirements in locust flight: lift to power ratio was reduced by 12% with the dynamic camber removed and by 35% with camber and twist removed (Young et al. 2009). A similar study on hover fly wings produced similar (but more modest) results, with the removal of camber deformations reducing lift production by 10% and the removal of wing twisting increasing power requirements by 5% (Du and Sun 2010). Examination of butterfly wings revealed the strongest effects yet; lift to power ratio was reduced by 4% with camber removed and by 46% with wing twist and camber removed (Zheng et al. 2013). Overall, these computational results show that deformation improves the aerodynamic performance of insect wings and that wing twist tends to have a greater effect than wing camber.

In contrast to the rapid advances in computational modeling techniques, experimental approaches to directly testing the effects of wing deformations on live insects have been hindered by the technical challenges associated with altering the flexibility of delicate, ultralight insect wings without significantly altering their mass and resulting flapping dynamics. However, the recent identification of resilin in the vein joints of many insect wings has opened up the possibility of performing experimental studies in vivo, as manipulating the stiffness of these small, isolated patches can affect wing stiffness significantly while adding minimal mass. This approach was adopted recently in a study testing the effects of wing stiffness on maximum force production in bumblebees via an asymptotic load-lifting test. A microsplint was applied to a single resilin joint, significantly increasing chordwise wing stiffness with minimal effect on mass, and leading to an average decrease in vertical force production of 8.5% (Mountcastle and Combes 2013). These experimental results support the findings of prior computational models showing that wing flexibility improves aerodynamic force output.

Sensing and control of insect flight

The small size of flying insects leaves them vulnerable to environmental perturbations. To make matters worse, most flying insects are unstable and a mild perturbation could grow to a wild oscillation in only a few wingbeats if not corrected. Thus, exquisite neurosensory and control capabilities are required to enable even the most basic of flight tasks. Recently, progress in understanding these capabilities and their source has come from two directions: (1) increasingly sophisticated aerodynamic analyses that better predict the stability of insects to different perturbations and (2) new experimental methods that control the visual sensory input received by free-flying animals independent of their actual speed or orientation.

Aerodynamics of flight stability and control

Improvements in computational capabilities and numerical approaches to fluid modeling recently reached the point at which numerical studies of insect flight can provide estimates of the forces and torques produced throughout the wingbeat cycles, and how these forces and torques would respond to a change in the insect's state such as a slight increase in forward velocity or pitching velocity (Sun and Lan 2004). Results from such studies allow for a linearized stability analysis similar to that used earlier to interpret the response of tethered locusts to changes in pitch orientation (Taylor and Thomas 2003). The emerging consensus from these analyses (Sun and Lan 2004; Sun and Wang 2007; Sun et al. 2009) shows that insects are dynamically unstable in pitch,

but the rate of growth in the instability is slow, typically 4–20 wingbeats. This instability generally takes the following form: (*i*) the insect pitches up slightly, this redirects some of the aerodynamic force from the wings rearward; (*ii*) this rearward force accelerates the insect backward; (*iii*) drag from the wings of the backward-moving animal creates a forward pitch torque; (*iv*) the insect pitches forward, directing aerodynamic force forward and producing forward acceleration; (*v*) drag on the wings of the forward-moving insect creates an upward pitch torque, beginning the oscillation again. Continued improvements to numerical simulation methods are now pushing into lateral stability (Zhang and Sun 2010; Gao et al. 2011) and nonlinear stability (Wu and Sun 2012) analysis methods.

Despite advancements in computational speed, numerical methods remain difficult to generalize among species. This challenge has led to searches for analytic approximations to animal flight stability that can be easily tuned to the morphology and kinematics of different species, allowing predictions of flight dynamics for animals across a range of sizes and shapes. These analyses revealed that although flapping flight is dynamically unstable in pitch, it also provides passive stability in yaw (Hedrick et al. 2009), making flying insects more stable than a traditional, single-rotor helicopter of the same scale. Because the analytic models depend on only a few measures of morphology and kinematics, they are easily extended to a wide range of flying animals and showed that larger animals are less stable in yaw than smaller flying animals, but not as much less as predicted by isometric scaling (Hedrick 2011). Further work on analytic stability models has extended them to other degrees of freedom and flight modes (Faruque and Sean Humbert 2010*a*, 2010*b*; Cheng et al. 2011; Ristroph et al. 2013).

Experimental advances in flight stability and control

Perhaps the most important overall findings from all the aforementioned stability analyses, computational or analytical, is the role movement plays in flight control. For example, the instability in pitch is actually driven by coupling between horizontal motion and pitch torque. Similarly, passive stability in yaw described above arises from the interaction between flapping motion and whole-body yaw rotation. Thus, experimental examination of insect flight control sensing and response need to incorporate motion damping and gain consistent with the biomechanics of the animal in question. The most straightforward means for accomplishing this is analysis of unrestrained flight maneuvers performed by freely behaving animals, using a combination of the "expected" response of the animal calculated from CFD or mechanical simulation results and the "observed" response taken from the experiment to identify the neurosensory control contribution (Cheng et al. 2011). However, these simple free-flight experiments do not allow manipulation of the visual environment, restricting the range of flight conditions and sensory inputs over which the insect's response can be recorded. Carrying out free-flight experiments in arenas with computer-controlled visual environments (e.g., Kern et al. 2005; Mronz and Lehmann 2008) or simply varying the visual environment (e.g., Barron and Srinivasan 2006) goes some distance toward alleviating these problems; for a further review of these systems see Taylor et al. (2008). However, recent technological advances now allow coupling of real-time quantification of the free-flight behavior of an insect and a computer-controlled visual environment (Fig. 11), offering the best of both worlds by preserving the free-flight dynamics of the insect while also allowing manipulation of the sensory input to probe the flight control responses across a wide range of conditions (Fry et al. 2009; Rohrseitz and Fry 2011). One of the most interesting results from these studies lies in the unexpected linear relationships discovered between visual sensory inputs and insect responses. Since both aerodynamics and visual information processing contain a number of nonlinear components, the combination of the two was expected to produce a highly nonlinear result. However, at least in some cases the aerodynamic and sensory nonlinear effects counteract one another, resulting in a simple and linear control response over a wide range of conditions (Medici and Fry 2013).

Sensing and stability

Although visual sensory systems are of great importance in determining some aspects of insect flight control, vision is far from the only important sensory mode. The long neural processing times associated with vision can lead to sensory delays of up to several wingbeats (Theobald 2004), which may be inadequate to control flight in cases where the doubling time of a perturbation is also only a few wingbeats, as was found in some of the numerical stability analyses mentioned above. Instead, insects also make use of mechanical gyroscopes to provide low-latency information on body orientation. The halteres of dipterans are a well-known example (Pringle 1957), but the ubiquitous pitch instability of flapping insect flight makes it likely that other groups also have their own means of rapidly sensing body rotations. Recent evidence indicates that the antenna play such a role in hawkmoths and possibly other Lepidoptera (Sane et al. 2007). Insects may also use conservative perturbation response strategies that avoid overresponding to sensory information acquired with a large latency (Cheng et al. 2011).

Maneuverability

The intrinsic instability of flapping flight facilitates maneuverability in insects to the extent that a vast number of different adjustments to the wing kinematics can produce the same type of maneuver (Hedrick and Daniel 2006; Dickson et al. 2010). Nevertheless, application of modern high-speed video recording and analysis tools have revealed a number of different wing-motion asymmetries used to produce different types of maneuver. For instance, hawkmoths modulate long axis wing rotation during pitch maneuvers (Cheng et al. 2011) and change wing trajectory to perform yaw turns (Hedrick and Robinson 2010). Furthermore, recent attempts to associate free-flight maneuvers with underlying variation in the neuromuscular activation of the flight muscles has shown that the division of labor between large flight power muscles and small maneuvering muscles is less than absolute, and flight power muscles are clearly implicated in the maneuvers of hawkmoths (Wang et al. 2008; Springthorpe et al. 2012). The development of exceptionally lightweight, animal portable neural signal amplifiers and transmitters (Ando et al. 2002) will likely permit many such associations between neuromuscular inputs, wing kinematics, and free-flight maneuvers in the near future.

In addition to simple changes in wing trajectory, insects may also maneuver by changing the passive properties of the wing, indirectly creating force asymmetries between left and right wings by engaging the aeroelastic and inertial shape changes characteristic of flapping wings. A recent study of free-flight yaw turns in fruit flies (Bergou et al. 2010) suggests just such as a mechanism, with a slight change in the effective tension of the torsional stiffness of the wing base resulting in left–right asymmetries in wing long axis rotation and a yaw maneuver. Such mechanisms may be widespread and uncovering them will require an integrative understanding of insect flight dynamics, flexible wing aerodynamics, the structure of the wing base and muscle attachments, and the neuromuscular inputs to these muscles.

Evolution of insect flight

The evolutionary origin of insect flight remains unknown and research in this area proceeds more slowly than in the previously described physiological and biomechanical aspects of insect flight, where new experimental and computational techniques have produced many advances in understanding. However, discovery of directed aerial descent in rainforest canopy ant species (Yanoviak et al. 2005) revealed the possibility of gliding and aerial behaviors

Fig. 11. The TrackFly open and closed loop flight arena used by Fry et al. (2009; modified and reproduced with permission of J. Exp. Biol., vol. 212, issue 8, ©2009 The Company of Biologists Ltd.). The arena includes a wind tunnel with flow direction shown by the blue arrows (A), a two-camera real-time tracking system (green arrows; B), and a computer projector with a set of mirrors (yellow arrows; C) creating a virtual reality visual pattern on the wind-tunnel walls. Flies generally flew upwind (red broken line; D) at a speed determined by the interaction of airspeed and visual-pattern speed. Figure appears in colour on the Web.

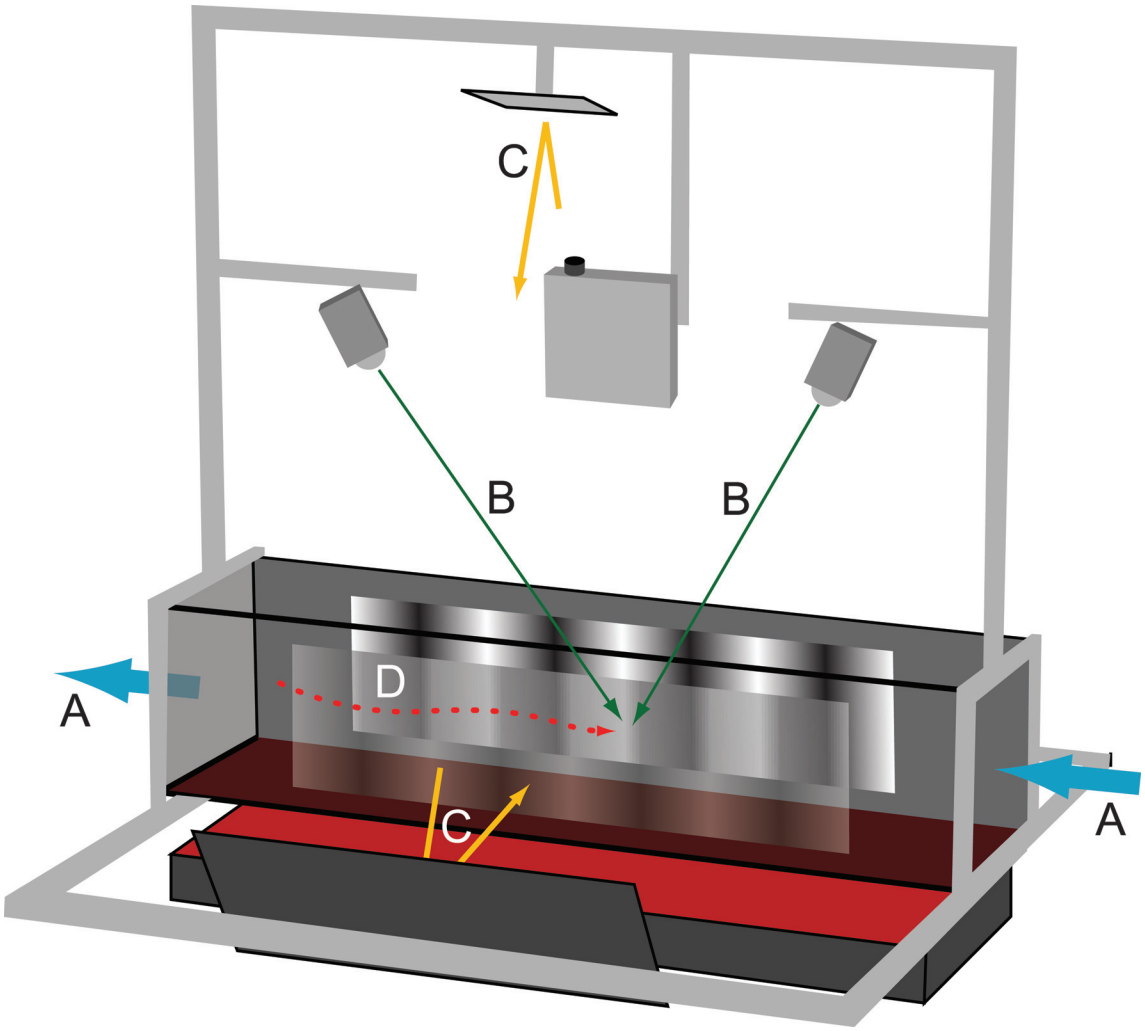

in wingless insects. This supports a functional origin of insect flight via gliding (Yanoviak et al. 2009), as opposed to the previously popular skimming model (Marden and Kramer 1994). However, directed aerial descent does not address the morphological origin of the insect wing; a recent evolution of development study of insect wing formation suggests a complex origin incorporating developmental modules from the limbs and body wall (Niwa et al. 2010). This developmental program may correspond to wing-like dorsal structures identified on the thoracic and abdominal segments of 300-million-year-old insect fossils (Kukalova-Peck 1978), which are suppressed in modern insect development but may be reactivated by RNA interference on *Hox* genes in larval insects (Ohde et al. 2013).

Further reading

Several of the topics presented in this brief review have recently been the subject of book-length reviews that provide far more depth and detail in the relevant areas. In particular, Dudley (2000) covered the biomechanics of insect flight, touching on many of the topic areas presented here and others such as the diversity of flying insects and evolution of insect flight. Vigoreaux (2006) reviewed insect flight muscle, while Taylor and Krapp (2007) along with Floreano et al. (2009) examined insect sensing and flight control.

Acknowledgements

We thank two anonymous reviewers for their comments that greatly improved this review.

References

Acheson, D.J. 1990. Elementary fluid dynamics. Oxford University Press, Oxford, UK.

Adrian, R.J. 2005. Twenty years of particle image velocimetry. Exp. Fluids, **39**(2): 159–169. doi:10.1007/s00348-005-0991-7.

Agianian, B., Kržič, U., Qiu, F., Linke, W.A., Leonard, K., and Bullard, B. 2004. A troponin switch that regulates muscle contraction by stretch instead of calcium. EMBO J. **23**(4): 772–779. doi:10.1038/sj.emboj.7600097. PMID:14765112.

Alben, S. 2009. Wake-mediated synchronization and drafting in coupled flags. J. Fluid Mech. **641**: 489–496. doi:10.1017/S0022112009992138.

Alben, S., and Shelley, M. 2005. Coherent locomotion as an attracting state for a free flapping body. Proc. Natl. Acad. Sci. U.S.A. **102**(32): 11163–11166. doi:10.1073/pnas.0505064102. PMID:16055551.

Alexander, D.E. 1984. Unusual phase relationships between the forewings and hindwings in flying dragonflies. J. Exp. Biol. **109**(1): 379–383.

Altshuler, D.L., Dickson, W.B., Vance, J.T., Roberts, S.P., and Dickinson, M.H. 2005. Short-amplitude high-frequency wing strokes determine the aerody-

namics of honeybee flight. Proc. Natl. Acad. Sci. U.S.A. **102**(50): 18213–18218. doi:10.1073/pnas.0506590102. PMID:16330767.
Ando, N., Shimoyama, I., and Kanzaki, R. 2002. A dual-channel FM transmitter for acquisition of flight muscle activities from the freely flying hawkmoth, *Agrius convolvuli*. J. Neurosci. Methods, **115**(2): 181–187. doi:10.1016/S0165-0270(02)00013-4. PMID:11992669.
Askew, G.N., Tregear, R.T., and Ellington, C.P. 2010. The scaling of myofibrillar actomyosin ATPase activity in apid bee flight muscle in relation to hovering flight energetics. J. Exp. Biol. **213**(7): 1195–1206. doi:10.1242/jeb.034330. PMID:20228356.
Barron, A., and Srinivasan, M.V. 2006. Visual regulation of ground speed and headwind compensation in freely flying honey bees (*Apis mellifera* L.). J. Exp. Biol. **209**(5): 978–984. doi:10.1242/jeb.02085. PMID:16481586.
Batchelor, G.K. 1967. An introduction to fluid dynamics. Cambridge University Press, Cambridge, UK.
Bergou, A.J., Xu, S., and Wang, Z.J. 2007. Passive wing pitch reversal in insect flight. J. Fluid Mech. **591**: 321–337. doi:10.1017/S0022112007008440.
Bergou, A.J., Ristroph, L., Guckenheimer, J., Cohen, I., and Wang, Z.J. 2010. Fruit flies modulate passive wing pitching to generate in-flight turns. Phys. Rev. Lett. **104**(14): 148101. doi:10.1103/PhysRevLett.104.148101. PMID:20481964.
Bhalla, A.P.S., Bale, R., Griffith, B.E., and Patankar, N.A. 2013. A unified mathematical framework and an adaptive numerical method for fluid–structure interaction with rigid, deforming, and elastic bodies. J. Comput. Phys. **250**: 446–476. doi:10.1016/j.jcp.2013.04.033.
Birch, J.M., and Dickinson, M.H. 2001. Spanwise flow and the attachment of the leading-edge vortex on insect wings. Nature, **412**(6848): 729–733. doi:10.1038/35089071. PMID:11507639.
Birch, J.M., and Dickinson, M.H. 2003. The influence of wing–wake interactions on the production of aerodynamic forces in flapping flight. J. Exp. Biol. **206**(13): 2257–2272. doi:10.1242/jeb.00381. PMID:12771174.
Birch, J.M., Dickson, W.B., and Dickinson, M.H. 2004. Force production and flow structure of the leading edge vortex on flapping wings at high and low Reynolds numbers. J. Exp. Biol. **207**(7): 1063–1072. doi:10.1242/jeb.00848. PMID:14978049.
Bomphrey, R., Lawson, N., Taylor, G., and Thomas, A. 2006. Application of digital particle image velocimetry to insect aerodynamics: measurement of the leading-edge vortex and near wake of a Hawkmoth. Exp. Fluids, **40**(4): 546–554. doi:10.1007/s00348-005-0094-5.
Bomphrey, R.J., Taylor, G.K., and Thomas, A.L.R. 2010. Smoke visualization of free-flying bumblebees indicates independent leading-edge vortices on each wing pair. *In* Animal locomotion. *Edited by* G.K. Taylor, M.S. Triantafyllou, and C. Tropea. Springer-Verlag, Berlin. pp. 249–259.
Bomphrey, R.J., Henningsson, P., Michaelis, D., and Hollis, D. 2012. Tomographic particle image velocimetry of desert locust wakes: instantaneous volumes combine to reveal hidden vortex elements and rapid wake deformation. J. R. Soc. Interface, **9**(77): 3378–3386. doi:10.1098/rsif.2012.0418.
Bullard, B., Leonard, K., Larkins, A., Butcher, G., Karlik, C., and Fyrberg, E. 1988. Troponin of asynchronous flight muscle. J. Mol. Biol. **204**(3): 621–637. doi:10.1016/0022-2836(88)90360-9. PMID:2852258.
Cartar, R.V. 1992. Morphological senescence and longevity: an experiment relating wing wear and life span in foraging wild bumble bees. J. Anim. Ecol. **61**(1): 225–231. doi:10.2307/5525.
Chen, K.K., Colonius, T., and Taira, K. 2010. The leading-edge vortex and quasisteady vortex shedding on an accelerating plate. Phys. Fluids, **22**(3): 033601–033611. doi:10.1063/1.3327282.
Cheng, B., Deng, X., and Hedrick, T.L. 2011. The mechanics and control of pitching manoeuvres in a freely flying hawkmoth (*Manduca sexta*). J. Exp. Biol. **214**(24): 4092–4106. doi:10.1242/jeb.062760. PMID:22116752.
Chi, K.J., Chang, C.T., Wu, M.H., and Shih, M.C. 2012. Enigma of pterostigma: an inertial regulator for deformation in flapping wings in dragonflies. *In* Society for Experimental Biology Annual Meeting, Salzburg, Austria, 29 June to 2 July 2012. The Society for Experimental Biology, London, UK.
Cloupeau, M., Devillers, J.F., and Devezeaux, D. 1979. Direct measurements of instantaneous lift in desert locust; comparison with Jensen's experiments on detached wings. J. Exp. Biol. **80**(1): 1–15.
Combes, S.A., and Daniel, T.L. 2003*a*. Flexural stiffness in insect wings I. Scaling and the influence of wing venation. J. Exp. Biol. **206**(17): 2979–2987. doi:10.1242/jeb.00523.
Combes, S.A., and Daniel, T.L. 2003*b*. Flexural stiffness in insect wings II. Spatial distribution and dynamic wing bending. J. Exp. Biol. **206**(17): 2989–2997. doi:10.1242/jeb.00524.
Combes, S.A., and Daniel, T.L. 2003*c*. Into thin air: Contributions of aerodynamic and inertial–elastic forces to wing bending in the hawkmoth *Manduca sexta*. J. Exp. Biol. **206**(17): 2999–3006. doi:10.1242/jeb.00502. PMID:12878668.
Combes, S.A., Crall, J.D., and Mukherjee, S. 2010. Dynamics of animal movement in an ecological context: dragonfly wing damage reduces flight performance and predation success. Biol. Lett. **6**(3): 426–429. doi:10.1098/rsbl.2009.0915. PMID:20236968.
Daniel, T.L., and Combes, S.A. 2002. Flexible wings and fins: bending by inertial or fluid-dynamic forces? Integr. Comp. Biol. **42**(5): 1044–1049. doi:10.1093/icb/42.5.1044. PMID:21680386.
Dickinson, M.D., and Gotz, K.G. 1993. Unsteady aerodynamic performance of model wings at low Reynolds numbers. J. Exp. Biol. **174**(1): 45–64.
Dickinson, M.H., Lehmann, F.-O., and Sane, S.P. 1999. Wing rotation and the aerodynamic basis of insect flight. Science, **284**(5422): 1881–2044. doi:10.1126/science.284.5422.1954.
Dickinson, M., Farman, G., Frye, M., Bekyarova, T., Gore, D., Maughan, D., and Irving, T. 2005. Molecular dynamics of cyclically contracting insect flight muscle in vivo. Nature, **433**(7023): 330–334. doi:10.1038/nature03230. PMID:15662427.
Dickson, W.B., and Dickinson, M.H. 2004. The effect of advance ratio on the aerodynamics of revolving wings. J. Exp. Biol. **207**(24): 4269–4281. doi:10.1242/jeb.01266. PMID:15531648.
Dickson, W.B., Polidoro, P., Tanner, M.M., and Dickinson, M.H. 2010. A linear systems analysis of the yaw dynamics of a dynamically scaled insect model. J. Exp. Biol. **213**(17): 3047–3061. doi:10.1242/jeb.042978. PMID:20709933.
Donoughe, S., Crall, J.D., Merz, R.A., and Combes, S.A. 2011. Resilin in dragonfly and damselfly wings and its implications for wing flexibility. J. Morphol. **272**(12): 1409–1421. doi:10.1002/jmor.10992. PMID:21915894.
Du, G., and Sun, M. 2010. Effects of wing deformation on aerodynamic forces in hovering hoverflies. J. Exp. Biol. **213**(13): 2273–2283. doi:10.1242/jeb.040295. PMID:20543126.
Dudley, R. 2000. The biomechanics of insect flight. Form, function, evolution. Princeton University Press, Princeton, N.J.
Dukas, R., and Dukas, L. 2011. Coping with nonrepairable body damage: effects of wing damage on foraging performance in bees. Anim. Behav. **81**(3): 635–638. doi:10.1016/j.anbehav.2010.12.011.
Elimelech, Y., Kolomenskiy, D., Dalziel, S.B., and Moffatt, H.K. 2013. Evolution of the leading-edge vortex over an accelerating rotating wing. Procedia IUTAM, **7**: 233–242. doi:10.1016/j.piutam.2013.03.027.
Ellington, C.P. 1995. Unsteady aerodynamics of insect flight. Symp. Soc. Exp. Biol. **49**: 109–129. PMID:8571220.
Ellington, C.P. 1999. The novel aerodynamics of insect flight: applications to micro-air vehicles. J. Exp. Biol. **202**(23): 3439–3448. PMID:10562527.
Ellington, C.P., van den Berg, C., Willmott, A.P., and Thomas, A.L.R. 1996. Leading-edge vortices in insect flight. Nature, **384**(6610): 626–630. doi:10.1038/384626a0.
Elsinga, G.E., Scarano, F., Wieneke, B., and van Oudheusden, B.W. 2006. Tomographic particle image velocimetry. Exp. Fluids, **41**(6): 933–947. doi:10.1007/s00348-006-0212-z.
Ennos, A.R. 1988. The importance of torsion in the design of insect wings. J. Exp. Biol. **140**(1): 137–160.
Ennos, A.R. 1989. Inertial and aerodynamic torques on the wings of Diptera in flight. J. Exp. Biol. **142**(1): 87–95.
Ennos, A.R. 1995. Mechanical behaviour in torsion of insect wings, blades of grass and other cambered structures. Proc. R. Soc. B Biol. Sci. **259**(1354): 15–18. doi:10.1098/rspb.1995.0003.
Faruque, I., and Sean Humbert, J. 2010*a*. Dipteran insect flight dynamics. Part 1: Longitudinal motion about hover. J. Theor. Biol. **264**(2): 538–552. doi:10.1016/j.jtbi.2010.02.018. PMID:20170664.
Faruque, I., and Sean Humbert, J. 2010*b*. Dipteran insect flight dynamics. Part 2: Lateral–directional motion about hover. J. Theor. Biol. **265**(3): 306–313. doi:10.1016/j.jtbi.2010.05.003. PMID:20470783.
Fernández, M.J., Springthorpe, D., and Hedrick, T.L. 2012. Neuromuscular and biomechanical compensation for wing asymmetry in insect hovering flight. J. Exp. Biol. **215**(20): 3631–3638. doi:10.1242/jeb.073627. PMID:22771747.
Floreano, D., Zufferey, J.-C., Srinivasan, M.V., and Ellington, C. (*Editors*). 2009. Flying insects and robots. Springer-Verlag, Berlin and Heidelberg.
Foster, D.J., and Cartar, R.V. 2011. What causes wing wear in foraging bumble bees? J. Exp. Biol. **214**(11): 1896–1901. doi:10.1242/jeb.051730. PMID:21562177.
Fry, S.N., Rohrseitz, N., Straw, A.D., and Dickinson, M.H. 2009. Visual control of flight speed in *Drosophila melanogaster*. J. Exp. Biol. **212**(8): 1120–1130. doi:10.1242/jeb.020768. PMID:19329746.
Fuchiwaki, M., Kuroki, T., Tanaka, K., and Tababa, T. 2013. Dynamic behavior of the vortex ring formed on a butterfly wing. Exp. Fluids, **54**(1): 1–12. doi:10.1007/s00348-012-1450-x.
Gao, N., Aono, H., and Liu, H. 2011. Perturbation analysis of 6DoF flight dynamics and passive dynamic stability of hovering fruit fly *Drosophila melanogaster*. J. Theor. Biol. **270**(1): 98–111. doi:10.1016/j.jtbi.2010.11.022. PMID:21093456.
George, N.T., Irving, T.C., Williams, C.D., and Daniel, T.L. 2013. The cross-bridge spring: can cool muscles store elastic energy? Science, **340**(6137): 1217–1220. doi:10.1126/science.1229573. PMID:23618763.
Gorb, S.N. 1999. Serial elastic elements in the damselfly wing: mobile vein joints contain resilin. Naturwissenschaften, **86**(11): 552–555. doi:10.1007/s001140050674. PMID:10551953.
Griffith, B.E., and Peskin, C.S. 2005. On the order of accuracy of the immersed boundary method: higher order convergence rates for sufficiently smooth problems. J. Comput. Phys. **208**(1): 75–105. doi:10.1016/j.jcp.2005.02.011.
Haas, F., Gorb, S., and Blickhan, R. 2000*a*. The function of resilin in beetle wings. Proc. R. Soc. B Biol. Sci. **267**(1451): 1375–1381. doi:10.1098/rspb.2000.1153.
Haas, F., Gorb, S., and Wootton, R.J. 2000*b*. Elastic joints in dermapteran hind wings: materials and wing folding. Arthropod Struct. Dev. **29**(2): 137–146.
Hedrick, T.L. 2011. Damping in flapping flight and its implications for manoeuvring, scaling and evolution. J. Exp. Biol. **214**(24): 4073–4081. doi:10.1242/jeb.047001. PMID:22116750.

Hedrick, T.L., and Daniel, T.L. 2006. Flight control in the hawkmoth *Manduca sexta*: the inverse problem of hovering. J. Exp. Biol. **209**(16): 3114–3130. doi:10.1242/jeb.02363. PMID:16888060.

Hedrick, T.L., and Robinson, A.K. 2010. Within-wingbeat damping: dynamics of continuous free-flight yaw turns in *Manduca sexta*. Biol. Lett. **6**(3): 422–425. doi:10.1098/rsbl.2010.0083. PMID:20181557.

Hedrick, T.L., Cheng, B., and Deng, X. 2009. Wingbeat time and the scaling of passive rotational damping in flapping flight. Science, **324**(5924): 252–255. doi:10.1126/science.1168431. PMID:19359586.

Hou, G., Wang, J., and Layton, A. 2012. Numerical methods for fluid–structure interaction—a review. Comm. Comput. Phys. **12**: 337–377. doi:10.4208/cicp.291210.290411s.

Irving, T.C. 2006. X-ray diffraction of indirect flight muscle from *Drosophila* in vivo. *In* Nature's versatile engine: insect flight muscle inside and out. *Edited by* J.O. Vigoreaux. Springer Science+Business Media, New York. pp. 197–213.

Irving, T.C., and Maughan, D.W. 2000. In vivo x-ray diffraction of indirect flight muscle from *Drosophila melanogaster*. Biophys. J. **78**(5): 2511–2515. doi:10.1016/S0006-3495(00)76796-8. PMID:10777748.

Ishihara, D., Yamashita, Y., Horie, T., Yoshida, S., and Niho, T. 2009. Passive maintenance of high angle of attack and its lift generation during flapping translation in crane fly wing. J. Exp. Biol. **212**(23): 3882–3891. doi:10.1242/jeb.030684. PMID:19915131.

Iwamoto, H., Inoue, K., and Yagi, N. 2010. Fast x-ray recordings reveal dynamic action of contractile and regulatory proteins in stretch-activated insect flight muscle. Biophys. J. **99**(1): 184–192. doi:10.1016/j.bpj.2010.04.009. PMID:20655846.

Jin, T., Goo, N.S., Woo, S.-C., and Park, H.C. 2009. Use of a digital image correlation technique for measuring the material properties of beetle wing. J. Bionic Eng. **6**(3): 224–231. doi:10.1016/S1672-6529(08)60105-5.

Johansson, L.C., Engel, S., Baird, E., Dacke, M., Muijres, F.T., and Hedenström, A. 2012. Elytra boost lift, but reduce aerodynamic efficiency in flying beetles. J. R. Soc. Interface, **9**(75): 2745–2748. doi:10.1098/rsif.2012.0053. PMID:22593097.

Jones, A.R., and Babinsky, H. 2011. Reynolds number effects on leading edge vortex development on a waving wing. Exp. Fluids, **51**(1): 197–210. doi:10.1007/s00348-010-1037-3.

Josephson, R.K. 1985. Mechanical power output from striated muscle during cyclic contraction. J. Exp. Biol. **114**(1): 493–512.

Josephson, R.K., Malamud, J.G., and Stokes, D.R. 2000*a*. Asynchronous muscle: a primer. J. Exp. Biol. **203**(18): 2713–2722. PMID:10952872.

Josephson, R.K., Malamud, J.G., and Stokes, D.R. 2000*b*. Power output by an asynchronous flight muscle from a beetle. J. Exp. Biol. **203**(17): 2667–2689. PMID:10934007.

Josephson, R.K., Malamud, J.G., and Stokes, D.R. 2001. The efficiency of an asynchronous flight muscle from a beetle. J. Exp. Biol. **204**(23): 4125–4139. PMID:11809787.

Kern, R., van Hateren, J.H., Michaelis, C., Lindemann, J.P., and Egelhaaf, M. 2005. Function of a fly motion-sensitive neuron matches eye movements during free flight. PLoS Biol. **3**(6): e171. doi:10.1371/journal.pbio.0030171. PMID:15884977.

Kesel, A.B., Philippi, U., and Nachtigall, W. 1998. Biomechanical aspects of the insect wing: an analysis using the finite element method. Comp. Biol. Med. **28**(4): 423–437. doi:10.1016/S0010-4825(98)00018-3.

Kolomenskiy, D., Moffatt, H.K., Farge, M., and Schneider, K. 2011. Two- and three-dimensional numerical simulations of the clap–fling–sweep of hovering insects. J. Fluids Struct. **27**(5–6): 784–791. doi:10.1016/j.jfluidstructs.2011.05.002.

Krasny, R. 1986. Desingularization of periodic vortex sheet roll-up. J. Comput. Phys. **65**(2): 292–313. doi:10.1016/0021-9991(86)90210-X.

Krasny, R. 1991. Vortex sheet computations: roll-up, wakes, separation. Lect. Appl. Math. **28**(1): 385–401.

Kukalova-Peck, J. 1978. Origin and evolution of insect wings and their relation to metamorphosis, as documented by the fossil record. J. Morphol. **156**(1): 53–125. doi:10.1002/jmor.1051560104.

Lee, L., and LeVeque, R. 2003. An immersed interface method for incompressible Navier–Stokes equations. SIAM J. Sci. Comput. **25**(3): 832–856. doi:10.1137/S1064827502414060.

Lehmann, F.-O., Sane, S.P., and Dickinson, M. 2005. The aerodynamic effects of wing–wing interaction in flapping insect wings. J. Exp. Biol. **208**(16): 3075–3092. doi:10.1242/jeb.01744. PMID:16081606.

Lehmann, F.-O., Gorb, S., Nasir, N., and Schützner, P. 2011. Elastic deformation and energy loss of flapping fly wings. J. Exp. Biol. **214**(17): 2949–2961. doi:10.1242/jeb.045351. PMID:21832138.

Lentink, D., and Dickinson, M.H. 2009. Rotational accelerations stabilize leading edge vortices on revolving fly wings. J. Exp. Biol. **212**(16): 2705–2719. doi:10.1242/jeb.022269. PMID:19648415.

Lentink, D., Jongerius, S.R., and Bradshaw, N.L. 2009. The scalable design of flapping micro-air vehicles inspired by insect flight. *In* Flying insects and robots. *Edited by* D. Floreano, J.-C. Zufferey, M.V. Srinivasan, and C. Ellington. Springer-Verlag, Berlin and Heidelberg. pp. 185–205. doi:10.1007/978-3-540-89393-6.

Levy, R., Uminsky, D., Park, A., and Calambokidis, J. 2011. A theory for the hydrodynamic origin of whale flukeprints. Int. J. Non-Linear Mech. **46**(4): 616–626. doi:10.1016/j.ijnonlinmec.2010.12.009.

Li, Z., and Lai, M.-C. 2001. The immersed interface method for the Navier–Stokes equations with singular forces. J. Comput. Phys. **171**(2): 822–842. doi:10.1006/jcph.2001.6813.

Lighthill, M.J. 1973. On the Weis-Fogh mechanism of lift generation. J. Fluid Mech. **60**(1): 1–17. doi:10.1017/S0022112073000017.

Linari, M., Reedy, M.K., Reedy, M.C., Lombardi, V., and Piazzesi, G. 2004. Ca-activation and stretch-activation in insect flight muscle. Biophys. J. **87**(2): 1101–1111. doi:10.1529/biophysj.103.037374. PMID:15298914.

Liu, H. 2009. Integrated modeling of insect flight: from morphology, kinematics to aerodynamics. J. Comput. Phys. **228**(2): 439–459. doi:10.1016/j.jcp.2008.09.020.

Liu, H., Ellington, C.P., Kawachi, K., Van den Berg, C., and Willmott, A.P. 1998. A computational fluid dynamic study of hawkmoth hovering. J. Exp. Biol. **201**(4): 461–477. PMID:9438823.

Lu, Y., and Shen, G.X. 2008. Three-dimensional flow structures and evolution of the leading-edge vortices on a flapping wing. J. Exp. Biol. **211**(8): 1221–1230. doi:10.1242/jeb.010652. PMID:18375846.

Machin, K.E., and Pringle, J.W.S. 1960. The physiology of insect fibrillar muscle. III. The effect of sinusoidal changes of length on a beetle flight muscle. Proc. R. Soc. B Biol. Sci. **152**(948): 311–330. doi:10.1098/rspb.1960.0041. PMID:13853745.

Mao, S., and Xin, Y. 2003. Flows around two airfoils performing fling and subsequent translation and subsequent clap. Acta Mech. Sin. **19**(2): 103–117. doi:10.1007/BF02487671.

Marden, J.H., and Kramer, M.G. 1994. Surface-skimming stoneflies: a possible intermediate stage in insect flight evolution. Science, **266**(5184): 427–430. doi:10.1126/science.266.5184.427. PMID:17816688.

Maxworthy, T. 1979. Experiments on the Weis-Fogh mechanism of lift generation by insects in hovering flight. Part 1. Dynamics of the 'fling'. J. Fluid Mech. **93**(1): 47–63. doi:10.1017/S0022112079001774.

Maxworthy, T. 2007. The formation and maintenance of a leading-edge vortex during the forward motion of an animal wing. J. Fluid Mech. **587**: 471–475. doi:10.1017/S0022112007007616.

May, M.L. 1991. Dragonfly flight: power requirements at high speed and acceleration. J. Exp. Biol. **158**(1): 325–342.

Medici, V., and Fry, S.N. 2013. Embodied linearity of speed control in *Drosophila melanogaster*. J. R. Soc. Interface, **9**(77): 3260–3267. doi:10.1098/rsif.2012.0527.

Miller, L.A., and Peskin, C.S. 2004. When vortices stick: an aerodynamic transition in tiny insect flight. J. Exp. Biol. **207**(17): 3073–3088. doi:10.1242/jeb.01138. PMID:15277562.

Miller, L.A., and Peskin, C.S. 2005. A computational fluid dynamics of 'clap and fling' in the smallest insects. J. Exp. Biol. **208**(2): 195–212. doi:10.1242/jeb.01376. PMID:15634840.

Miller, L.A., and Peskin, C.S. 2009. Flexible clap and fling in tiny insect flight. J. Exp. Biol. **212**(19): 3076–3090. doi:10.1242/jeb.028662. PMID:19749100.

Miller, L.A., Goldman, D.I., Hedrick, T.L., Tytell, E.D., Wang, Z.J., Yen, J., and Alben, S. 2012. Using computational and mechanical models to study animal locomotion. Integr. Comp. Biol. **52**(5): 553–575. doi:10.1093/icb/ics115. PMID:22988026.

Milne-Thomson, L.M. 1966. Theoretical aerodynamics. Dover Publications, New York.

Mittal, R., and Iaccarino, G. 2005. Immersed boundary methods. Annu. Rev. Fluid Mech. **37**: 239–261. doi:10.1146/annurev.fluid.37.061903.175743.

Mittal, R., Dong, H., Bozkurttas, M., Najjar, F.M., Vargas, A., and von Loebbecke, A. 2008. A versatile sharp interface immersed boundary method for incompressible flows with complex boundaries. J. Comput. Phys. **227**(10): 4825–4852. doi:10.1016/j.jcp.2008.01.028. PMID:20216919.

Mountcastle, A.M., and Combes, S.A. 2013. Wing flexibility enhances load-lifting capacity in bumblebees. Proc. R. Soc. B Biol. Sci. **280**(1759). doi:10.1098/rspb.2013.0531.

Mountcastle, A.M., and Combes, S.A. 2014. Biomechanical strategies for mitigating collision damage in insect wings: structural design versus embedded elastic materials. J. Exp. Biol. **217**(7): 1108–1115. doi:10.1242/jeb.092916. PMID:24311806.

Mountcastle, A., and Daniel, T. 2009. Aerodynamic and functional consequences of wing compliance. Exp. Fluids, **46**(5): 873–882. doi:10.1007/s00348-008-0607-0.

Mronz, M., and Lehmann, F.-O. 2008. The free-flight response of *Drosophila* to motion of the visual environment. J. Exp. Biol. **211**(13): 2026–2045. doi:10.1242/jeb.008268. PMID:18552291.

Nachtigall, W. 1981. Hydromechanics and biology. Biophys. Struct. Mech. **8**(1–2): 1–22. doi:10.1007/BF01047102. PMID:7326353.

Nachtigall, W. 2000. Abbiegungen und Abknickungen von Insektenflügeln beim Flug ohne und mit zusätzlicher Beutelast. [Insect wing bending and folding during flight without and with an additional prey load.] Entomol. Gen. **25**(1): 1–16. [In German.] doi:10.1127/entom.gen/25/2000/1.

Nakata, T., and Liu, H. 2012*a*. Aerodynamic performance of a hovering hawkmoth with flexible wings: a computational approach. Proc. R. Soc. B Biol. Sci. **279**(1729): 722–731. doi:10.1098/rspb.2011.1023.

Nakata, T., and Liu, H. 2012*b*. A fluid–structure interaction model of insect flight with flexible wings. J. Comput. Phys. **231**(4): 1822–1847. doi:10.1016/j.jcp.2011.11.005.

Newman, D.J.S., and Wootton, R.J. 1986. An approach to the mechanics of pleating in dragonfly wings. J. Exp. Biol. **125**(1): 361–372.

Newman, J.C., III, Newman, P.A., Taylor, A.C., III, and Hou, G.J.-W. 1999. Efficient

nonlinear static aeroelastic wing analysis. Comp. Fluids, **28**(4–5): 615–628. doi:10.1016/S0045-7930(98)00047-4.
Niwa, N., Akimoto-Kato, A., Niimi, T., Tojo, K., Machida, R., and Hayashi, S. 2010. Evolutionary origin of the insect wing via integration of two developmental modules. Evol. Dev. **12**(2): 168–176. doi:10.1111/j.1525-142X.2010.00402.x. PMID: 20433457.
Norberg, R.Å. 1972. The pterostigma of insect wings an inertial regulator of wing pitch. Comp. Physiol. A, **81**(1): 9–22.
Ohde, T., Yaginuma, T., and Niimi, T. 2013. Insect morphological diversification through the modification of wing serial homologs. Science, **340**(6131): 495–498. doi:10.1126/science.1234219. PMID:23493422.
Perz-Edwards, R.J., Irving, T.C., Baumann, B.A.J., Gore, D., Hutchinson, D.C., Kržič, U., Porter, R.L., Ward, A.B., and Reedy, M.K. 2011. X-ray diffraction evidence for myosin–troponin connections and tropomyosin movement during stretch activation of insect flight muscle. Proc. Natl. Acad. Sci. U.S.A. **108**(1): 120–125. doi:10.1073/pnas.1014599107. PMID:21148419.
Pesavento, U., and Wang, Z.J. 2009. Flapping wing flight can save aerodynamic power compared to steady flight. Phys. Rev. Lett. **103**(11): 118102. doi:10.1103/PhysRevLett.103.118102. PMID:19792403.
Peskin, C.S. 1972. Flow patterns around heart valves: a numerical method. J. Comput. Phys. **10**(2): 252–271. doi:10.1016/0021-9991(72)90065-4.
Peskin, C.S. 2002. The immersed boundary method. Acta Numerica, **11**: 479–517. doi:10.1017/S0962492902000077.
Phillips, N., and Knowles, K. 2013. Formation of the leading-edge vortex and spanwise flow on an insect-like flapping-wing throughout a flapping half cycle. *Edited by* CERES. Cranfield University, Cranfield, Bedfordshire, UK.
Pringle, J.W.S. 1949. The excitation and contraction of the flight muscles of insects. J. Physiol. (Lond.), **108**(2): 226–232.
Pringle, J.W.S. 1957. Insect flight. Cambridge University Press, London.
Ramamurti, R., and Sandberg, W.C. 2007. A computational investigation of the three-dimensional unsteady aerodynamics of *Drosophila* hovering and maneuvering. J. Exp. Biol. **210**(5): 881–896. doi:10.1242/jeb.02704. PMID:17297147.
Rees, C.J.C. 1975. Form and function in corrugated insect wings. Nature, **256**: 200–203. doi:10.1038/256200a0.
Ristroph, L., Ristroph, G., Morozova, S., Bergou, A.J., Chang, S., Guckenheimer, J., Wang, Z.J., and Cohen, I. 2013. Active and passive stabilization of body pitch in insect flight. J. R. Soc. Interface, **10**(85): 20130237. doi:10.1098/rsif.2013.0237.
Rival, D., Schönweitz, D., and Tropea, C. 2011. Vortex interaction of tandem pitching and plunging plates: a two-dimensional model of hovering dragonfly-like flight. Bioinspiration Biomimetics, **6**(1): 016008. doi:10.1088/1748-3182/6/1/016008. PMID:21335652.
Rohrseitz, N., and Fry, S.N. 2011. Behavioural system identification of visual flight speed control in *Drosophila melanogaster*. J. R. Soc. Interface, **8**(55): 171–185. doi:10.1098/rsif.2010.0225.
Sane, S.P. 2003. The aerodynamics of insect flight. J. Exp. Biol. **206**: 4191–4208. doi:10.1242/jeb.00663. PMID:14581590.
Sane, S.P., and Dickinson, M.H. 2002. The aerodynamic effects of wing rotation and a revised quasi-steady model of flapping flight. J. Exp. Biol. **205**: 1087–1096. PMID:11919268.
Sane, S.P., Dieudonné, A., Willis, M.A., and Daniel, T.L. 2007. Antennal mechanosensors mediate flight control in moths. Science, **315**(5813): 863–866. doi:10.1126/science.1133598. PMID:17290001.
Shukla, R.K., and Eldredge, J.D. 2007. An inviscid model for vortex shedding from a deforming body. Theor. Comput. Fluid Dyn. **21**(5): 343–368. doi:10.1007/s00162-007-0053-2.
Smith, C.W., Herbert, R., Wootton, R.J., and Evans, K.E. 2000. The hind wing of the desert locust (*Schistocerca gregaria* Forskål). II. Mechanical properties and functioning of the membrane. J. Exp. Biol. **203**(19): 2933–2943. PMID: 10976030.
Song, D., Wang, H., Zeng, L., and Yin, C. 2001. Measuring the camber deformation of a dragonfly wing using projected comb fringe. Rev. Sci. Instrum. **72**(5): 2450–2454. doi:10.1063/1.1364664.
Song, F., Lee, K.L., Soh, A.K., Zhu, F., and Bai, Y.L. 2004. Experimental studies of the material properties of the forewing of cicada (Homoptera, Cicàdidae). J. Exp. Biol. **207**(17): 3035–3042. doi:10.1242/jeb.01122. PMID:15277558.
Song, F., Xiao, K.W., Bai, K., and Bai, Y.L. 2007. Microstructure and nanomechanical properties of the wing membrane of dragonfly. Mater. Sci. Eng. A, **457**(1–2): 254–260. doi:10.1016/j.msea.2007.01.136.
Springthorpe, D., Fernández, M.J., and Hedrick, T.L. 2012. Neuromuscular control of free-flight yaw turns in the hawkmoth *Manduca sexta*. J. Exp. Biol. **215**(10): 1766–1774. doi:10.1242/jeb.067355. PMID:22539744.
Srygley, R.B., and Thomas, A.L.R. 2002. Unconventional lift-generating mechanisms in free-flying butterflies. Nature, **420**(6916): 660–664. doi:10.1038/nature01223. PMID:12478291.
Sun, M., and Lan, S.L. 2004. A computational study of the aerodynamic forces and power requirements of dragonfly (*Aeschna juncea*) hovering. J. Exp. Biol. **207**(11): 1887–1901. doi:10.1242/jeb.00969. PMID:15107443.
Sun, M., and Tang, J. 2002. Unsteady aerodynamic force generation by a model fruit fly wing in flapping motion. J. Exp. Biol. **205**(1): 55–70. PMID:11818412.
Sun, M., and Wang, J.K. 2007. Flight stabilization control of a hovering model insect. J. Exp. Biol. **210**(15): 2714–2722. doi:10.1242/jeb.004507. PMID:17644686.
Sun, M., Liu, Y.P., and Wang, J.K. 2009. Dynamic flight stability of a hovering hoverfly. *In* New trends in fluid mechanics research. *Edited by* F.G. Zhuang and J.C. Li. Springer-Verlag, Berlin and Heidelberg. pp. 626–629.
Sunada, S., Zeng, L., and Kawachi, K. 1998. The relationship between dragonfly wing structure and torsional deformation. J. Theor. Biol. **193**(1): 39–45. doi:10.1006/jtbi.1998.0678.
Sunada, S., Song, D., Meng, X., Wang, H., Zeng, L., and Kawachi, K. 2002*a*. Optical measurement of the deformation, motion, and generated force of the wings of a moth, *Mythimna separata* (Walker). JSME Int. J. Ser. B Fluids Therm. Eng. **45**(4): 836–842. doi:10.1299/jsmeb.45.836.
Sunada, S., Takashima, H., Hattori, T., Yasuda, K., and Kawachi, K. 2002*b*. Fluid-dynamic characteristics of a bristled wing. J. Exp. Biol. **205**(17): 2737–2744. PMID:12151379.
Tangorra, J.L., Lauder, G.V., Hunter, I.W., Mittal, R., Madden, P.G.A., and Bozkurttas, M. 2010. The effect of fin ray flexural rigidity on the propulsive forces generated by a biorobotic fish pectoral fin. J. Exp. Biol. **213**(23): 4043–4054. doi:10.1242/jeb.048017. PMID:21075946.
Taylor, G.K., and Krapp, H.G. 2007. Sensory systems and flight stability: what do insects measure, and why? *In* Insect mechanics and control. *Edited by* J. Casas and S.J. Simpson. Academic Press, London. pp. 231–316.
Taylor, G.K., and Thomas, A.L.R. 2003. Dynamic flight stability in the desert locust *Schistocerca gregaria*. J. Exp. Biol. **206**(16): 2803–2829. doi:10.1242/jeb.00501. PMID:12847126.
Taylor, G.K., Bacic, M., Bomphrey, R.J., Carruthers, A.C., Gillies, J., Walker, S.M., and Thomas, A.L.R. 2008. New experimental approaches to the biology of flight control systems. J. Exp. Biol. **211**(2): 258–266. doi:10.1242/jeb.012625. PMID:18165253.
Theobald, J.C. 2004. Perceiving motion in the dark. Ph.D. dissertation, University of Washington, Seattle.
Thomas, A.L.R., Taylor, G.K., Srygley, R.B., Nudds, R.L., and Bomphrey, R.J. 2004. Dragonfly flight: free-flight and tethered flow visualizations reveal a diverse array of unsteady lift-generating mechanisms, controlled primarily via angle of attack. J. Exp. Biol. **207**(24): 4299–4323. doi:10.1242/jeb.01262. PMID: 15531651.
Tu, M.S., and Daniel, T.L. 2004. Submaximal power output from the dorsolongitudinal flight muscles of the hawkmoth *Manduca sexta*. J. Exp. Biol. **407**(26): 4651–4662. doi:10.1242/jeb.01321.
Usherwood, J.R., and Ellington, C.P. 2002. The aerodynamics of revolving wings I. Model hawkmoth wings. J. Exp. Biol. **205**: 1547–1564. PMID:12000800.
Usherwood, J.R., and Lehmann, F.-O. 2008. Phasing of dragonfly wings can improve aerodynamic efficiency by removing swirl. J. R. Soc. Interface, **5**(28): 1303–1307. doi:10.1098/rsif.2008.0124.
Van den Berg, C., and Ellington, C.P. 1997. The three-dimensional leading-edge vortex of a 'hovering' model hawkmoth. Philos. Trans. R. Soc. B Biol. Sci. **352**(1351): 329–340. doi:10.1098/rstb.1997.0024.
Vandenberghe, N., Zhang, J.U.N., and Childress, S. 2004. Symmetry breaking leads to forward flapping flight. J. Fluid Mech. **506**: 147–155. doi:10.1017/S0022112004008468.
Vanella, M., Fitzgerald, T., Preidikman, S., Balaras, E., and Balachandran, B. 2009. Influence of flexibility on the aerodynamic performance of a hovering wing. J. Exp. Biol. **212**(1): 95–105. doi:10.1242/jeb.016428. PMID:19088215.
Vigoreaux, J.O. (*Editor*). 2006. Nature's versatile engine: insect flight muscle inside and out. Springer Science+Business Media, New York.
Vincent, J.F.V., and Wegst, U.G.K. 2004. Design and mechanical properties of insect cuticle. Arthropod Struct. Dev. **33**(3): 187–199. doi:10.1016/j.asd.2004.05.006. PMID:18089034.
Vogel, S. 1967. Flight in *Drosophila* III. Aerodynamic characteristics of fly wings and wing models. J. Exp. Biol. **46**(3): 431–443.
Walker, S.M., Thomas, A.L.R., and Taylor, G.K. 2009*a*. Deformable wing kinematics in the desert locust: how and why do camber, twist and topography vary through the stroke? J. R. Soc. Interface, **6**(38): 735–747. doi:10.1098/rsif.2008.0435.
Walker, S.M., Thomas, A.L.R., and Taylor, G.K. 2009*b*. Photogrammetric reconstruction of high-resolution surface topographies and deformable wing kinematics of tethered locusts and free-flying hoverflies. J. R. Soc. Interface, **6**(33): 351–366. doi:10.1098/rsif.2008.0245.
Walker, S.M., Thomas, A.L.R., and Taylor, G.K. 2010. Deformable wing kinematics in free-flying hoverflies. J. R. Soc. Interface, **7**(42): 131–142. doi:10.1098/rsif.2009.0120.
Walker, S.M., Thomas, A.L.R., and Taylor, G.K. 2012. Operation of the alula as an indicator of gear change in hoverflies. J. R. Soc. Interface, **9**(71): 1194–1207. doi:10.1098/rsif.2011.0617.
Walker, S.M., Schwyn, D.A., Mokso, R., Wicklein, M., Müller, T., Doube, M., Stampanoni, M., Krapp, H.G., and Taylor, G.K. 2014. In vivo time-resolved microtomography reveals the mechanics of the blowfly flight motor. PLoS Biol. **12**(3): e1001823. doi:10.1371/journal.pbio.1001823. PMID:24667677.
Wang, H., Zeng, L., Liu, H., and Yin, C. 2003. Measuring wing kinematics, flight trajectory and body attitude during forward flight and turning maneuvers in dragonflies. J. Exp. Biol. **206**(4): 745–757. doi:10.1242/jeb.00183. PMID: 12517991.
Wang, H., Ando, N., and Kanzaki, R. 2008. Active control of free flight manoeuvres in a hawkmoth, *Agrius convolvuli*. J. Exp. Biol. **211**(3): 423–432. doi:10.1242/jeb.011791. PMID:18203998.

Wang, Z.J. 2000. Vortex shedding and frequency selection in flapping flight. J. Fluid Mech. **410**: 323–341. doi:10.1017/S0022112099008071.
Wang, Z.J. 2004. The role of drag in insect hovering. J. Exp. Biol. **207**(23): 4147–4155. doi:10.1242/jeb.01239. PMID:15498960.
Wang, Z.J., and Russell, D. 2007. Effect of forewing and hindwing interactions on aerodynamic forces and power in hovering dragonfly flight. Phys. Rev. Lett. **99**(14): 148101. doi:10.1103/PhysRevLett.99.148101. PMID:17930724.
Wang, Z.J., Birch, J.M., and Dickinson, M.H. 2004. Unsteady forces and flows in low Reynolds number hovering flight: two-dimensional computations vs robotic wing experiments. J. Exp. Biol. **207**(3): 449–460. doi:10.1242/jeb.00739. PMID:14691093.
Weis-Fogh, T. 1973. Quick estimates of flight fitness in hovering animals, including novel mechanisms for lift production. J. Exp. Biol. **59**(1): 169–230.
Wiens, J.K., and Stockie, J.M. 2015. An efficient parallel immersed boundary algorithm using a pseudo-compressible fluid solver.J. Comput. Phys. **281**: 917–941. doi:10.1016/j.jcp.2014.10.058.
Willert, C.E., and Gharib, M. 1991. Digital particle image velocimetry. Exp. Fluids, **10**(4): 181–193. doi:10.1007/BF00190388.
Willmott, A.P., and Ellington, C.P. 1997. The mechanics of flight in the hawkmoth *Manduca sexta*. I. Kinematics of hovering and forward flight. J. Exp. Biol. **200**(21): 2705–2722.
Wootton, R.J. 1979. Function, homology and terminology in insect wings. Syst. Entomol. **4**(1): 81–93. doi:10.1111/j.1365-3113.1979.tb00614.x.
Wootton, R.J. 1992. Functional morphology of insect wings. Annu. Rev. Entomol. **37**(1): 113–140. doi:10.1146/annurev.en.37.010192.000553.
Wootton, R.J. 1993. Leading edge section and asymmetric twisting in the wings of flying butterflies (Insecta, Papilionoidea). J. Exp. Biol. **180**(1): 105–117.
Wootton, R.J., Evans, K.E., Herbert, R., and Smith, C.W. 2000. The hind wing of the desert locust (*Schistocerca gregaria* Forskål). I. Functional morphology and mode of operation. J. Exp. Biol. **203**(19): 2921–2931. PMID:10976029.
Wu, J.H., and Sun, M. 2012. Floquet stability analysis of the longitudinal dynamics of two hovering model insects. J. R. Soc. Interface, **9**(74): 2033–2046. doi:10.1098/rsif.2012.0072.
Xu, S., and Wang, Z.J. 2006. An immersed interface method for simulating the interaction of a fluid with moving boundaries. J. Comput. Phys. **216**(2): 454–493. doi:10.1016/j.jcp.2005.12.016.
Yanoviak, S.P., Dudley, R., and Kaspari, M. 2005. Directed aerial descent in canopy ants. Nature, **433**(7026): 624–626. doi:10.1038/nature03254. PMID:15703745.
Yanoviak, S.P., Kaspari, M., and Dudley, R. 2009. Gliding hexapods and the origins of insect aerial behaviour. Biol. Lett. **5**(4): 510–512. doi:10.1098/rsbl.2009.0029. PMID:19324632.
Yilmaz, T.O., and Rockwell, D. 2011. Flow structure on finite-span wings due to pitch-up motion. J. Fluid Mech. **691**: 518–545. doi:10.1017/jfm.2011.490.
Young, J., Walker, S.M., Bomphrey, R.J., Taylor, G.K., and Thomas, A.L.R. 2009. Details of insect wing design and deformation enhance aerodynamic function and flight efficiency. Science, **325**(5947): 1549–1552. doi:10.1126/science.1175928. PMID:19762645.
Zanker, J.M., and Gotz, K.G. 1990. The wing beat of *Drosophila melanogaster*. II. Dynamics. Philos. Trans. R. Soc. B Biol. Sci. **327**(1238): 19–44. doi:10.1098/rstb.1990.0041.
Zeng, L., Matsumoto, H., and Kawachi, K. 1996. A fringe shadow method for measuring flapping angle and torsional angle of a dragonfly wing. Meas. Sci. Technol. **7**(5): 776. doi:10.1088/0957-0233/7/5/009.
Zeng, L., Hao, Q., and Kawachi, K. 2000. A scanning projected line method for measuring a beating bumblebee wing. Opt. Commun. **183**(1–4): 37–43. doi:10.1016/S0030-4018(00)00888-9.
Zhang, Y., and Sun, M. 2010. Dynamic flight stability of a hovering model insect: lateral motion. Acta Mech. Sin. **26**(2): 175–190. doi:10.1007/s10409-009-0303-1.
Zhao, L., Huang, Q., Deng, X., and Sane, S.P. 2010. Aerodynamic effects of flexibility in flapping wings. J. R. Soc. Interface, **7**(44): 485–497. doi:10.1098/rsif.2009.0200.
Zheng, H., McCauley, R., Schaeffer, S., and Xinyan, D. 2009. Aerodynamics of dragonfly flight and robotic design. *In* IEEE International Conference on Robotics and Automation (ICRA '09), Kobe, Japan, 12–17 May 2009.Institute of Electrical and Electronics Engineers (IEEE), New York. pp. 3061–3066. doi:10.1109/ROBOT.2009.5152760.
Zheng, L., Hedrick, T., and Mittal, R. 2013. A comparative study of the hovering efficiency of flapping and revolving wings. Bioinspiration Biomimetics, **8**(3): 036001. doi:10.1088/1748-3182/8/3/036001. PMID:23680659.